DESIGN AND CONSTRUCTION OF A TENSILE TESTER FOR THE TESTING OF SIMPLE COMPOSITES

Mark A. Borst

and

F. Xavier Spiegel

Loyola College
4501 N. Charles Street
Baltimore, Maryland 21210-2699

Telephone 410-617-5123 or 410-617-2515

Foreword

Materials testing has been an important part of engineering in America for over one hundred years. In 1832, the Franklin Institute began a systematic investigation into the cause of steam boiler explosions. This study was broken down into two parts. The first part was concerned with the operation of the boilers. The second part of the study, however, was concerned with the material used to construct the boilers. At the time, manufacturers of iron knew that their product was strong, but had no idea of how strong it was. The manufacture of iron was guided by rule of thumb and virtually nothing was measured. This ignorance concerning the production of iron did not have tremendous consequences until the arrival of the steam engine. Boilers proved the inadequacy of some irons by exploding violently. As a result, a method for testing materials was developed and initially executed by Walter R. Johnson, Professor of Mechanics and Natural Philosophy at The Franklin Institute in Philadelphia. This marked the first time that quantitative data on "proving tenacity" was gathered in America.[1]

Materials testing has grown considerably since Johnson's work and is now a major part of engineering. The material strength requirements for a steam engine pale in comparison to the requirements for the machines of today. From high speed electronic switches to space flight, the "boiler explosions" of today are much more costly, both in money and potential loss of life, than they were in Johnson's day. The explosion of the space shuttle Challenger is an example of the potential hazards waiting to happen. A single O-ring, cooled below an acceptable temperature, caused the loss of seven lives and billions of dollars. As a result, the strength and characteristics of a material must be fully understood before that material may be used in the manufacture of a product.

The following is a design for a tensile tester which will be used to test the tensile strength and anisotropic properties of simple composites. These simple composites are suspected to be anisotropic primarily in a single plane. When the composites undergo a tensile force, they will undergo deformation, causing movement either to the left or right. The composites are suspect due to their method of construction. Each sample has a single layer of unidirectional continuous fibers embedded in a rubbery resin. It has been well established that a serious limitation of unidirectional fiber composites is the very large in-plane anisotropy.[2]

The design presented here incorporates a single degree of freedom such that distortion (to the left or right) due to anisotropic tendencies may be measured. The device will spend the vast majority of its time in an undergraduate materials lab. As a result, ease of use and durability are valued more highly than research grade accuracy. Additional concerns focus on the fact that this machine will be built as a student project.

Issues which are dealt with during this design include:

1. Specimen configuration or shape.
2. Method of applying consistent, linear tension force.
3. Method of gripping specimen without affecting its overall properties.
4. Method of collecting data.
5. Repeatability of data.
6. Ease of use.
7. Ease of construction.
8. Cost.

After the device has been constructed, it will be used to test the simple composites which were fabricated in house. A comparison will be made between composites manufactured using aluminum screening as the strengthening fibers and those manufactured using fiberglass screening.

Design

Application of Force

The first matter which will be taken up is the application of force. A device is needed which can provide a consistent, linearly applied force, but still allow for lateral movement of the sample so that anisotropic properties as well as the modulus of elasticity and yield strength may be observed and measured. In addition, the machine must provide for an easy method by which several characteristics can be measured. These characteristics include:

1. Elongation
2. Lateral displacement as a result of anisotropic behavior.
3. Force applied.

A hand operated screw mechanism was chosen for the application of force. This provides a simple means of applying force in a single direction. In addition, the amount of force applied may be increased in a linear fashion with infinitesimal changes. The screw chosen was an Acme® threaded screw, one inch in diameter with a pitch of ten threads per inch. The Acme® thread is a square cut thread and is designed to support large amounts of force. This thread is commonly used in such high pressure applications as vices and large clamps. For each rotation of the screw, the sample will be elongated by one tenth of an inch. This provides a convenient point at which to take a reading of the force. As a result, measurements of force are taken every one tenth of an inch and the number of readings taken prove an accurate guide for the total elongation.

The screw is operated by means of a large hand wheel. The large wheel will provide leverage so that an adequate amount of torque may be easily applied to the screw which in turn will impart a large tensile force to the specimen which may be easily controlled by the operator.

In addition to being able to impart a tensile force to the sample, the screw must be able to support itself. This was accomplished by using a twenty inch long section of screw and turning down a one inch section on each end to 0.627" so that it would fit into two, flanged bushings. Figure 1 shows the hand wheel. Tensile force will be applied when the knob is turned clockwise. Most people associate a clockwise rotation of threaded objects with an application of force and hence operation of the wheel will be of second nature. The Acme® threaded rod appears in figure 2. Figure 3 shows the assembled screw mechanism. The screw and hand wheel are attached by means of a roll pin. A hole was drilled through the hand wheel and rod and the pin was then inserted.

Support and Load Transfer

Next to be considered is the frame of the machine. This is an important part since the frame not only supports the machine but facilitates the transfer of the load from the screw mechanism to the sample. In addition, it allows for lateral movement of the sample during testing. The frame is also the heart of the information gathering process. A load cell is mounted on the frame to allow for the measurement of the force being applied to the sample. The output from the load cell is read from a Fluke digital multimeter in milli-volts. Through information provided by the manufacturer as well as use of a standard, the relationship between the load cell's output in milli-volts to the actual pounds of force delivered was determined.

The support part of the frame was constructed from 1"x3" sections of maple (Note: These are mill dimensions). Maple was chosen because of its high strength and its beauty. The drive beam was constructed from oak. Maple would have been preferred, but a large enough piece was not available. The properties of these two woods appear in table 1 (all figures

refer to forces applied parallel to the grain). Poplar is included in the table since it is of sufficient strength to use in the construction of the frame and drive beam. In addition, relatively large poplar beams (4"x4") are readily available and poplar is less expensive than maple or oak. Unfortunately, poplar has a yellowish green tint that renders it much less pleasing to the eye than either oak or maple. One should never neglect the aesthetics of a design.

Wood	Specific Gravity	Modulus of Elasticity [lb/in^2 x 10^3]	Modulus of Rupture [lb/in^2]	Compressive Strength [lb/in^2]
Maple, sugar	0.676	1,830	15,500	7,800
Oak, white	0.710	1,770	15,100	7,440
Poplar, yellow	0.427	1,500	9,200	5,540

Table 1: Properties of selected hard woods.[3]

The frame was constructed by using carpenter's glue to laminate five pieces of maple together to form four beams. The sections were offset such that finger joints were formed at the corners. These beams were clamped tightly and the glue was allowed to dry. After the glue had dried, holes were drilled as required using a drill press and the appropriate bits. Figure 4 shows the construction of the support beams. The drive beam appears in figure 5. All parts must be assembled within the frame before any final gluing can take place. This includes two steel rods, as well as the drive beam itself and the Acme® rod with hand wheel in place. Once assembled, the frame was measured to check for squareness. It was racked into shape by use of large wood working clamps which mount on standard one inch diameter black pipe. Once the frame was squared, four 1/2" holes were drilled at each corner and four 1/2" hardwood dowels which had

been coated with glue were driven in place using a hammer. The resultant appears in figure 6 along with the two drive rods, rail assembly and mounted load cell.

The force from the drive beam is delivered to the sample by means of two, 36" long steel rods, 1" diameter. These drive rods support a rail and shuttle system which actually allows for the single degree of freedom. The rods have holes drilled in them such that the rail and shuttle system may be placed at different heights, thereby allowing for different length samples or grips (Figure 7).

A section of rail that was used appears in figure 8. The guide rail was commercially available in 6'-6" lengths. The rails were cut into four, 1'-3" sections and doubled as reinforcement to prevent any deformation during loading. The rails must remain straight if any anisotropic behavior is to be observed. If the rails bow, the shuttle system will remain in the trough of the bow. Figures 9 and 10 show how the rail assembly is constructed.

Grips and Shuttle system.

The grips were machined from aluminum and are straightforward in design. Each grip basically consists of a center, mounting plate and two gripping plates. The two gripping plates are fastened to either side of this center plate by means of four, knurled nuts. These nuts have four small holes on the knurled surface that allow for the insertion of a taper pin. This provides additional leverage in tightening the grips. The gripping plates were designed to be the exact same dimension as the sample to be tested. As a result, the plates alone are unable to grip the sample. This was done in order to minimize sample deformation from metal to composite clamping as this might affect the test. A thin sheet of rubber (obtained from the plumbing

section of a hardware store) was attached to the face of the gripping plates using Duro® contact cement. This allowed the clamping surface to conform somewhat to the sample as opposed to pinching it. To provide additional gripping ability, pieces of 3M's Press'n Sand® "Sticky back" sanding sheets were cut to size and affixed to the rubber faces. The gripping plates are the same for the top and bottom (Figure 11). The bottom grip (Figure 12) screws into the load cell (Figure 13).

The top grip consists of two gripping plates identical to those on the lower grip. These plates mount on a shuttle system. The shuttle system consists of a center plate and four guide wheels. The guide wheels were obtained from the same company which supplied the guide rail. The unassembled shuttle system appears in figure 14.

Some comments concerning the machine's operation might prove helpful in improving on the design. The grips were insufficient in holding the samples without the sandpaper faces, and even then loads peaked at a maximum of just over 100 pounds before the samples began to pull free from the grips. Also, the sandpaper faces slipped during tests and had to be replaced periodically. A better idea might be to alter the design to accept commercial grips. This may not alleviate all the problems. It was noticed that when a series of samples 1" wide were tested (to match the 1" wide samples being run on the Chatillon LDX tensile tester since its grips could accommodate nothing larger) anisotropic tendencies did not appear consistently. The 2.5" wide samples, however, displayed excellent anisotropic tendencies. Still, the commercial grips might be capable of delivering enough of a load to a 1" sample such that its anisotropic characteristics are revealed.

Calibration and Verification of Devices Functioning

The load cell was connected to a Fluke digital multimeter as per manufacturer's instructions. Using the load cell's specifications sheet, a relationship was determined between the load cell's output in milli-volts and the corresponding force in pounds. The relationship between the load cell's output in milli-volts and the tensile force applied was calculated to be:

$$Lbf = 998.84 \frac{Lbs}{volt} \times v \qquad \text{Equation 1}$$

Lbf = pounds force
v = volts

The first problem was that of collecting the data. After each full turn of the hand wheel (equivalent to an elongation of one tenth of an inch) the reading was taken from the multimeter and written down. In the time taken to write down the data, however, the sample had relaxed substantially. To prevent this, a small tape recorder was used to record data while the hand wheel was turned in a slow, constant fashion. This eliminated the problem of relaxation during data collection. Two people working together, as in an undergraduate lab, could also overcome the problem with one student turning the hand wheel and calling out the readings while the other student jots down the data.

The next problem encountered was the inaccuracy of the machine's output. Like samples of Ferris See-thru® (Neat, 0.3"x1"x5-3/4") were tested on the hand operated device and on a Chatillon LDX 500 pound capacity tensile tester. The data was off by an amount considered unacceptable (Figure 15). Two things are readily apparent in viewing figure 15. The first is that the hand operated device is reading ten pounds high (assuming the just purchased Chatillon was

correct). The second is that the slopes, or moduli of elasticity, are similar. It was suspected that since the samples were being subjected to less than 100 pounds force, that the 5000 pound capacity load cell simply was not in its most effective range. A small, 50 pound capacity hand held spring scale (similar to a "fish scale") was used to check this. First, the scale was checked for accuracy using the Chatillon. While the scale's readings fluctuated high and low with respect to the Chatillon's output, a series of ten trials running from zero to forty-four pounds yielded an average that was reasonably accurate (Figure 16). The scale was then attached to the hand operated device. Ten sets of readings were taken ranging from zero to forty-four pounds. The data was averaged, zeroed and plotted (Figure 17). The relationship between the load cell's output in milli-volts and pounds force was determined to be:

$$Lbf = \frac{mV - mV_0}{0.963} \qquad \text{Equation 2}$$

Figure 18 shows the comparison of the data from figure 15 using Equation 2. The fit is still not perfect, but it is closer. In addition, the two plots in figure 18 are closer to being parallel at values above 3/4 pounds. The modulus of elasticity was determined by determining the slope of a hand fitted line. The results are as follows:

Chatillon: $\frac{(24.62-0)Lbf}{(2-0)inches} = 12.31\frac{Lbf}{inch}$

Hand Operated: $\frac{(29.69-10.46)Lbf}{(2-0.5)inches} = 12.82\frac{Lbf}{inch}$

Difference: $\frac{(12.82-12.31)}{12.31} \times 100 = 4.14\%$

C-2

It is suspected that this small amount of error could be eradicated if a 500 pound load cell were used in the construction of the hand operated tensile tester. Unfortunately, none were available during the course of this project.

Samples

Many samples were tried during the course of working with this device. One inch wide samples were attractive at first because six were obtained from a single mold. Also, the Chatillon LDX's grips accepted nothing larger than a 1" sample. Unfortunately, 1" samples were very difficult to hold, slipping from the grips with as little as 40 pounds force. Also, the narrow span of fibers made the viewing of anisotropic properties difficult. Lateral displacement in samples which were obviously anisotropic was hit and miss. Data obtained from 1" samples will be ignored for the most part since like samples failed to respond in a consistent fashion.

Finally, 2.5" wide samples were used. The grips had originally been designed to hold samples of this size. The additional gripping surface proved invaluable, though slippage remained a problem throughout the tests. In addition, anisotropic properties were much more pronounced with the larger span of fibers. The bulk of data obtained from the 2.5" samples appears in the following brief discussion of tests.

Tests

The following is a series of eleven tests which were run on the completed and calibrated device. The composites which were tested were developed by M. D. Wampler and F. X. Spiegel of Loyola College, Maryland.[4] The original concept was modified by constructing a divider

which allowed for two, 0.3"x2.5"x5.75" samples to be constructed at a time. Aluminum and fiberglass screening were used for the strengthening fibers. Strands of screen were selectively removed to produce composites with continuous unidirectional fibers at different angles to the horizontal (0°, 30°, 45°, 60° and 90°). The bits of screen were removed using either a fine pair of scissors or a modeling knife. A single layer of fibers was used for each sample.

Sample test numbers consist of the date and the order in which the tests were performed on that date. The samples used were 0.3"x2.5"x5.75". Two plots accompany each test. The first plot is of pounds force versus elongation. The modulus of elasticity was calculated from these. The second plot is of lateral displacement versus elongation. If a sample is anisotropic, a shear strain will be produced when a tensile stress is applied.[5] The shuttle system used in supporting the top grip allows this shear stress to be expressed in movement either to the left or right.

Test #0716931 - Ferris See-thru® Neat (Figures 19 & 20).
Test #0716932 - Ferris See-thru® with aluminum fibers at 0° (horizontal) (Figures 21&22)
Test #0716933 - Ferris See-thru® with aluminum fibers at 30° (Figures 23 & 24).
Test #0716934 - Ferris See-thru® with aluminum fibers at 45° (Figures 25 & 26).
Test #0716935 - Ferris See-thru® with aluminum fibers at 60° (Figures 27 & 28).
Test #0716936 - Ferris See-thru® with aluminum fibers at 90° (vertical) (Figures 29 & 30).
Test #0716937 - Ferris See-thru® with fiberglass fibers at 0° (horizontal) (Figures 31 & 32).
Test #0716938 - Ferris See-thru® with fiberglass fibers at 30° (Figures 33 & 34).
Test #0716939 - Ferris See-thru® with fiberglass fibers at 45° (Figures 35 & 36).
Test #07169310 - Ferris See-thru® with fiberglass fibers at 60° (Figures 37 & 38).
Test #07169311 - Ferris See-thru® with fiberglass fibers at 90° (vertical) (Figures 39 & 40)

None of the samples tested were brought to failure. In the force versus elongation plots, the drop off is due to the sample slipping from the grips. While the force existing as the sample

slips from the grips is not important, what is important is the lateral displacement. Figures 26, 28, 30, 34, 36 and 38 clearly show the samples being laterally displaced as tension is applied. As the samples slipped from the grip, the lateral displacement reversed itself, with the samples moving back towards their original position. This data was retained since it further demonstrated the anisotropic properties of these composites.

Results

0716931 - Neat:

Modulus of Elasticity = $\frac{(48.22-20)Lbf}{(1.6-0.6)inch} = 28.22\frac{Lbf}{inch}$

The neat sample showed no surprises. It did not experience any permanent deformation, returning to its original dimensions after having slipped from the grips. The results appear in figures 19 and 20.

Aluminum

0716932 - Al fibers at 0° (Horizontal):

Modulus of Elasticity= $\frac{(58.57-0)Lbf}{(1.6-0)inch} = 36.60\frac{Lbf}{inch}$

The sample experienced some permanent deformation. Its final dimensions were 0.30"x2.42"x5.8". The aluminum wires were protruding from the sides of the sample as a result of the samples necking while under tension. It is believed that an uneven slippage rate of the aluminum wires caused the minimal amount of lateral displacement that was witnessed. The results appear in figures 21 and 22.

0716933 - Al fibers at 30°:

Modulus of Elasticity = $\frac{(62.57-0)Lbf}{(2-0)inch} = 31.29\frac{Lbf}{inch}$

The sample experienced some permanent deformation. Its final dimensions were 0.30"x2.48"x5.73". The aluminum wires were protruding from the sides of the sample as a result of the necking that occurred. In addition, the sample retained the shape of a parallelogram with an offset angle of 1°. The sample was originally 90° at the corner but has deviated to 89°. The results appear in figures 23 and 24.

0716934 - Al fibers at 45:

Modulus of Elasticity = $\frac{(59.43-0)Lbf}{(1.6-0)inch} = 37.14\frac{Lbf}{inch}$

The sample experienced permanent deformation. Its final dimensions were 0.30"x2.42"x5.80". The aluminum wires were protruding from the sides of the sample due to the necking which occurred while the sample was under tension. In addition, the sample overcompensated, returning slightly past its zero lateral displacement and retaining the shape of a parallelogram with an offset angle of 2.5° (87.5° at the corner). The results appear in figures 25 and 26.

0716935 - Al fibers at 60°:

Modulus of Elasticity = $\frac{(42.86-0)Lbf}{(0.75-0)inch} = 57.15\frac{Lbf}{inch}$

The sample experienced severe permanent deformation. Its final dimensions were 0.30"x2.40"x60". The aluminum wires were not protruding from the sides of the sample but there was a substantial amount of pull-out visible through the clear resin. In addition, the sample severely over compensated. As it slipped from the grips, it moved towards zero lateral

displacement. It overshot, however, and came to rest -0.200" away from zero deviation. Its offset angle was 11° (79° at corner). The results appear in figures 27 and 28.

0716936 - Al fibers at 90° (Vertical):

Modulus of Elasticity = $\frac{(94.55-0)Lbf}{(0.2-0)inch} = 472.73\frac{Lbf}{inch}$

The sample experienced severe permanent deformation. Its final dimensions were 0.30"x2.40"x6.00". The aluminum wires had suffered pull-out and were protruding from the broad flats of the sample. The lateral movement was caused by slack in the wires. This slack arose during fiber orientation during flow.[2] When the liquid Ferris See-thru® was poured over the fibers, they shifted position and took on a bowed shape. As the curve was pulled out of the bow, the sample shifted laterally. The results appear in figures 29 and 30.

Analysis

In measuring the modulus of elasticity, a line was hand fitted to each plot. An attempt was made to include only points which were measured before any slippage occurred. The modulus of elasticity is directly related to the stiffness of a material.[6] A high modulus of elasticity indicates that a large amount of force is required to elongate a specimen. The results obtained here showed that the sample with vertical fibers (90°) had the highest modulus of elasticity. This was expected since the aluminum fibers receive the entire load. It would have been expected that the composite with horizontal fibers (0°) would have had the lowest modulus of elasticity. This was not the case, according to the results. The sample with fibers at 30° had the lowest at 31.29 *Lbf/inch* as compared to 36.60 *Lbf/inch*. The validity of this result is in

question, but the percent error which was calculated during calibration does not account for it. The tendency of the samples to slip, however, would account for it.

The neat sample had the lowest modulus of elasticity of all. This was expected, since the chore of fibers within a composite is to provide strength while the resin's job is to support and protect the fibers.

It is suspected that the overcompensation displayed by the 45° and 60° aluminum was due to pull-out. Pull-out occurs when the fibers pull loose from the matrix.[2] Since the aluminum fibers are held in place by mechanical adhesion (mechanical interlocking of two surfaces) the bond between fiber and matrix is a weak one.[2] The hole left due to the pull-out of a fiber would neck down under tension, thus increasing the mechanical adhesion of the fiber. As the tension is released, the fiber does not slide entirely back into the hole from which it came. If this were the case, the array of aluminum fibers would now push the matrix in the opposite direction. This would explain the over compensation and the deformation which was so prominent in the 60° sample. Figure 41 shows a schematic of the distortion which took place in the aluminum fiber samples.

Fiberglass

0716937 - Fiberglass fibers at 0° (Horizontal):

Modulus of Elasticity = $\frac{(53.43-8.86)Lbf}{(1.6-0.2)inch} = 31.84\frac{Lbf}{inch}$

The sample experienced no permanent deformation. The fiberglass appears to have formed a more secure bond with the Ferris See-thru®. This was demonstrated by a lack of protrusion of fibers which was prevalent in the 0° with aluminum. The results appear in figures 31 and 32.

0716938 -Fiberglass fibers at 30°:

Modulus of Elasticity = $\frac{(55.43-10.86)Lbf}{(1.2-2)inch} = 44.57\frac{Lbf}{inch}$

The sample experienced some permanent deformation. Its dimensions remained the same, but it was offset by 1° (89° at the corner). Again, the fiberglass appears to have a more secure bond with the Ferris See-thru®. There was virtually no protrusion of fibers from the resin. The results appear in figures 33 and 34.

0716939 - Fiberglass fibers at 45°

Modulus of Elasticity = $\frac{(49.86-28.12)Lbf}{(0.8-0.4)inch} = 54.35\frac{Lbf}{inch}$

The sample experienced some permanent deformation. Its dimensions remained the same, but it was offset by 3° (87° at corner) due to over compensation. Again, the fiberglass appears to have a more secure bond with the Ferris See-thru®. This is demonstrated by a lack of protrusion of fibers which was more pronounced in the 45° with aluminum. The results appear in figures 35 and 36.

07169310 - Fiberglass fibers at 60°

Modulus of Elasticity = $\frac{(60-13.14)Lbf}{(0.8-0.2)inch} = 78.10\frac{Lbf}{inch}$

The sample experienced some permanent deformation. Its dimensions changed to 0.30"x2.42"x5.78". There was not as much offset due to over compensation as might be expected, only 2° (88° at corner). This is probably due to the comparably tenacious bond that the fiberglass fibers seem to have with the resin. The results appear in figures 37 and 38.

07169311 - Fiberglass fibers at 90°

Modulus of Elasticity = $\frac{(84.35-0)Lbf}{(0.2-0)inch} = 421.74\frac{Lbf}{inch}$

The sample experienced no permanent deformation, despite having experienced stresses in excess of one hundred pounds (by far the heaviest). The sample's dimensions remained the same and the fiberglass fibers showed no signs of pull-out. As with the aluminum at 90°, the lateral movement here is a result of fiber orientation during flow. The results appear in figures 39 and 40.

Analysis

The modulus of elasticity for the fiberglass composites behaved as expected with the 0° having the lowest modulus and the 90° having the highest. The composites whose fibers had higher angles of orientation had correspondingly higher moduli. This is as expected.

The fiberglass fibers form a bond with the resin that is far superior to the bond formed between the resin and aluminum fibers. The bond is still due to mechanical adhesion, but the fiberglass fibers have more surface rigosity. In addition, there are small "tabs" that remain on either side of the unidirectional fibers after the superfluous middle fibers are snipped free. This superior bond results in less sample deformation. Pull-out was virtually eliminated.

Overall, the fiberglass fibers proved superior to the aluminum fibers. Both pull-out and sample deformation were minimized with the use of fiberglass fibers. The aluminum was the stronger fiber, as evidenced by the modulus of elasticity for aluminum fibers arranged vertically. At 472.73 *Lbf inch*, it was 12% higher than the modulus of elasticity for the corresponding fiberglass sample. The aluminum sample, however, emerged from the test severely deformed while the fiberglass sample appeared unscathed.

Closing Comments

While the device designed and constructed during this course is useful, many improvements could be made to increase its usefulness as an educational instrument. Below are several suggestions.

1) The addition of two LVDT's, one to measure lateral displacement and one to measure necking.

2) The addition of a device which could collect data from the load cell, convert it to pounds force and store it.

3) A redesigned grip, based on the commercial grips used by Chatillon, but capable of holding 2.5" wide samples.

4) Replace the 5000 pound capacity load cell with a 500 pound capacity load cell.

These are only suggested modifications. In its current state, the device is simple to learn and provides reasonable results. The best results are obtained when people work in teams of two or three. This is especially the case when lateral displacement readings are being made. One person operates the hand wheel, reading off the voltages to a note taker. As each reading is taken, a third student can make measurements of the lateral displacement by means of a small ruler clipped on the rail assembly.

Acknowledgments

Finally, in closing, we would like to thank all those who contributed time and advice during the design, construction, and testing of this device: special thanks to Walter Krug and Mike Francoviac, who were so helpful with advice concerning the machining of the grips; Bob Borst, whose woodworking tools and skill were invaluable; John Ward, who aided in the actual operation of the completed device. We could not have accomplished so much in so little time without their help.

List of materials used in the construction of this device.

1. Machinist's Labor (approximately 40 hours) $1000
2. Guide Rail A7C15-3065, one 6.5' section at $55.60
   from Stock Drive Products
3. Guide Wheel A7Q16-2, four at $25.51
   from Stock Drive Products
5. Flanged Bushing - 0.627" inner diameter, O.D. 0.878", Length 1",
   two at $2.04 from Stock Drive Products, A 7B 4-SF202808

---

6. Alloy Steel Fully threaded rods, 1/2" -13, one at $4.78
   McMaster-Carr, 98957A636
7. Alloy Steel Fully threaded rods, 1/2"-20, one at $8.75
   McMaster-Carr, 92580A111
8. Round Drill Rod, 1/4", 3' long, one at $2.29
   McMaster-Carr, 8893K36.
9. Steel Rod, 3/8" dia., 12" length, one at $5.95
   McMaster-Carr, 6061K32
10. Guide Rod - 1" diameter, 20" length, two at $8.00
    from McMaster-Carr
11. Load Rod - 1" diameter, 36" length, two at $12.00
    from McMaster-Carr
12. Acme® threaded rod - 1" - 10 threads, 6' length, one at $55.00
    from McMaster-Carr, 98935A219

13. Acme® Carbon Steel Flange - 1" -flange dia. 2.760", mounting hole dia. 0.266", from McMaster-Carr, 95082A644, $28.00

14. Acme® Bronze round nut, 1" - 10 threads, outer dia. 1.5", length 1.5" McMaster-Carr, 95072A116, $28.00

15. Knurled nut, 1/2"-13, four at $3.58
McMaster-Carr, 94775A033

16. Cast Iron Hand Wheel - 10" outer dia., 2-1/4" tall, 2-1/4" dia. cntr. 1" dia. grip, McMaster-Carr, 6025K14, $29.38

17. Lumber and other materials obtained from hardware stores, $100.00

Total cost of construction = $1478.19

Suppliers:

McMaster-Carr Supply Company
Dayton, New Jersey
TEL. (908) 329-6666
FAX. (908) 329-3772

Stock Drive Products
Box 5416
New Hyde Park NY 11042-5416
(516) 328-3300

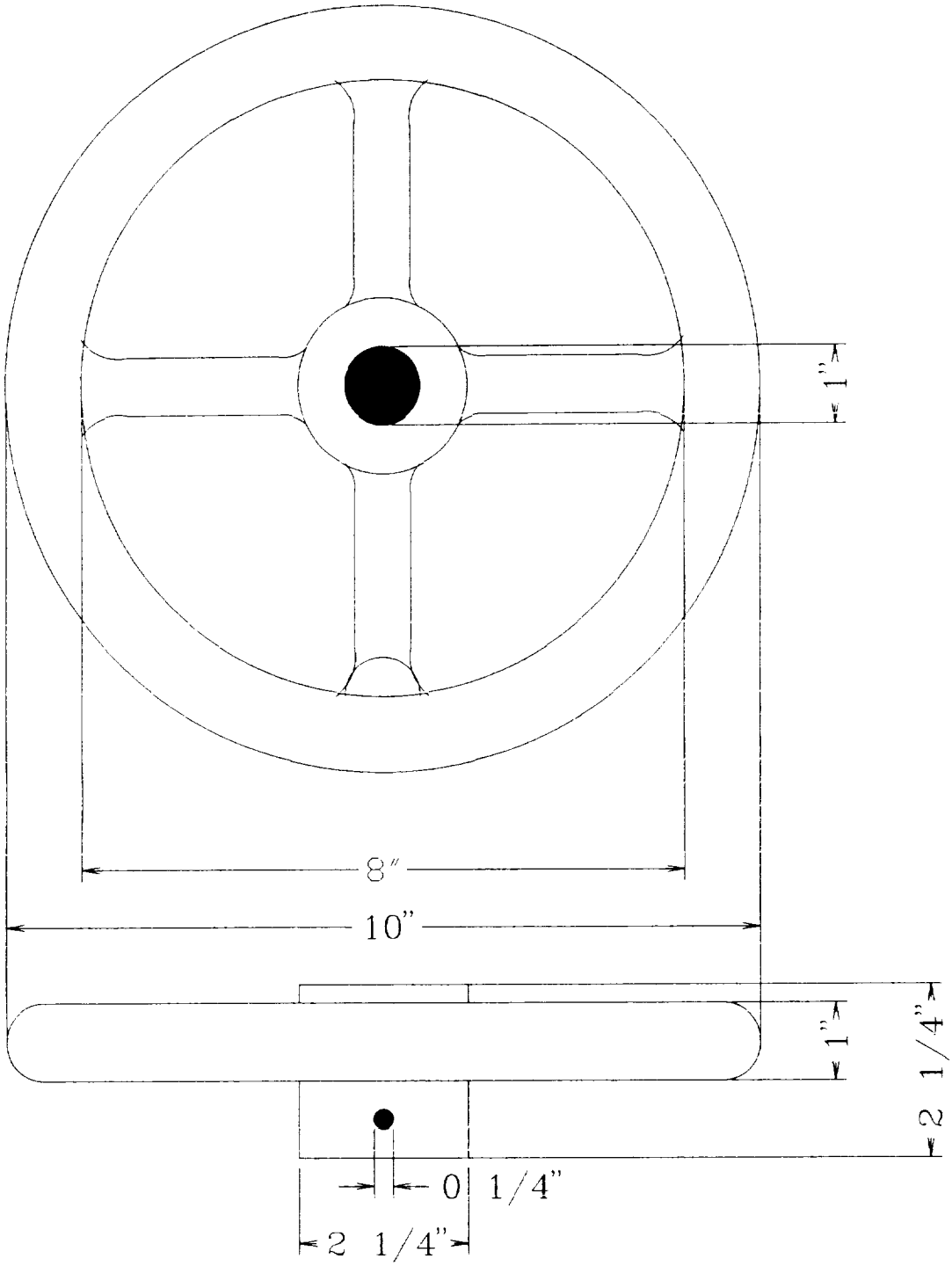

Figure 1. Hand wheel with through holes for Acme rod and roll pin.

Drive rod (1"-10) with ends turned down to 5/8".

Attach to hand wheel with roll pin four inches from bottom.

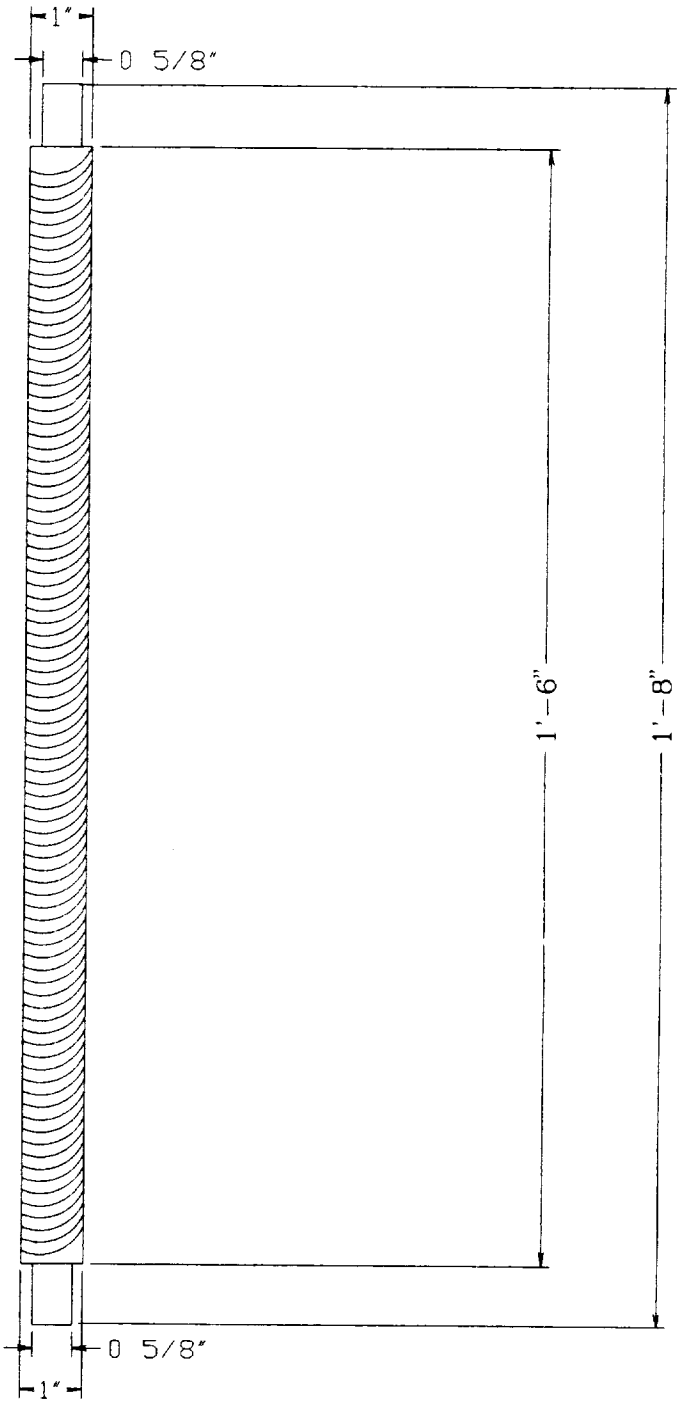

Figure 2. Acme threaded rod with ends turned down.

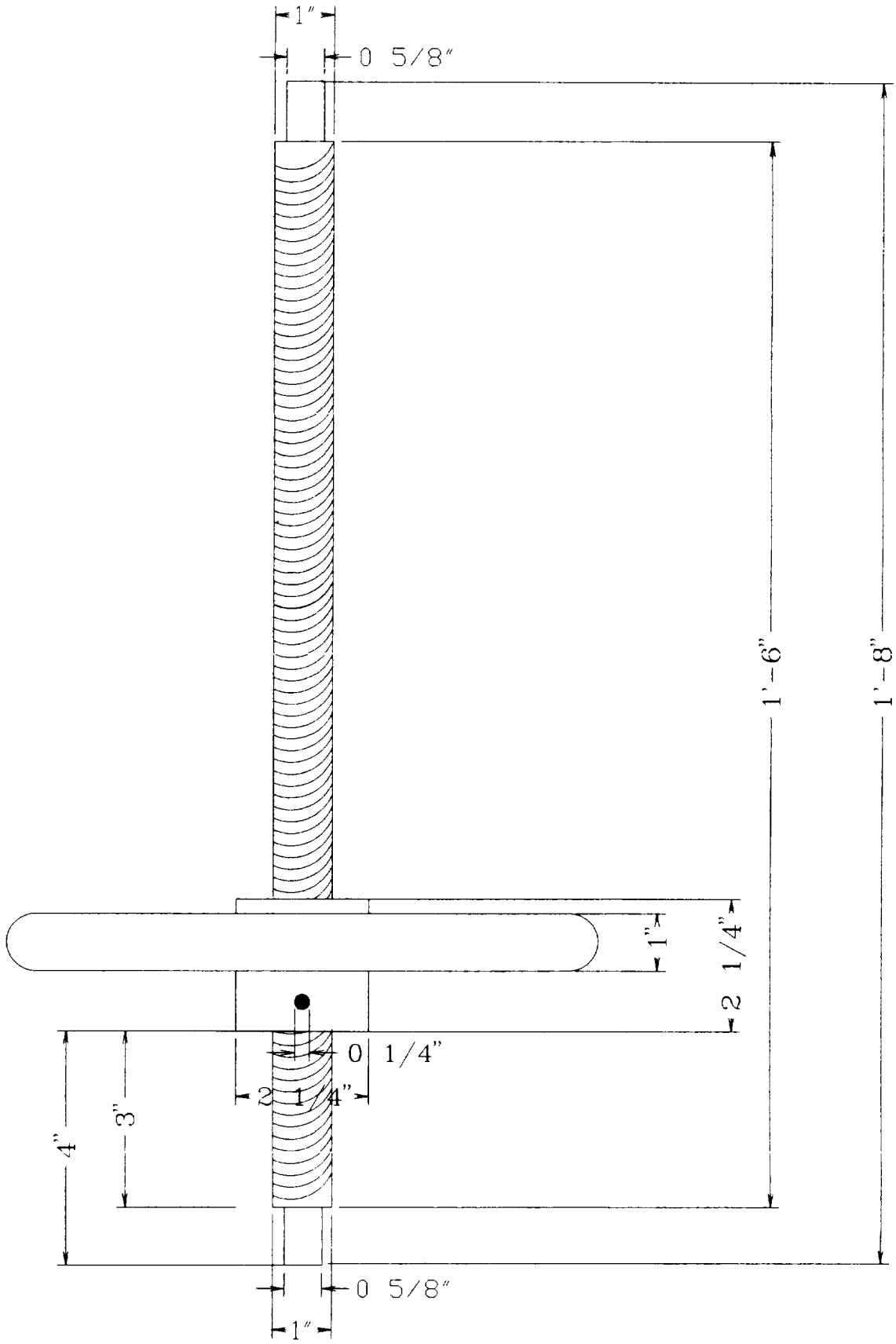

Figure 3. Acme threaded rod with hand wheel.

Laminated maple beam. Construct two horizontal beams with dimensions at right. Construct two vertical beams with the dimensions below.

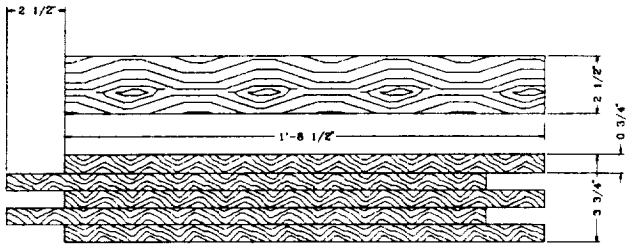

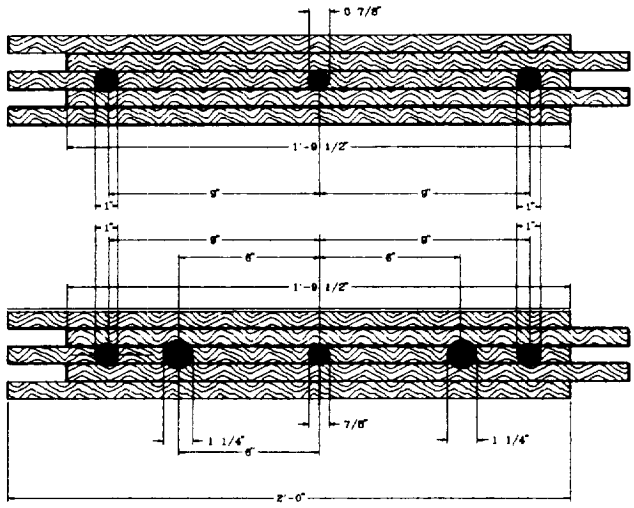

Top side of lower horizontal beam. All three holes are only 1" deep. The outer holes accept the 1" dia. guide rods while the center hole accepts the bushing which the Acme screw will ride in.

Under side of upper horizontal beam. The two outer holes, in addition to the center hole, are the same as on the lower, horizontal beam. The two 1 1/4" dia. holes that are 6" off center go all the way through the beam, allowing for passage of the two drive rods.

Figure 4. Construction of laminated maple beams.

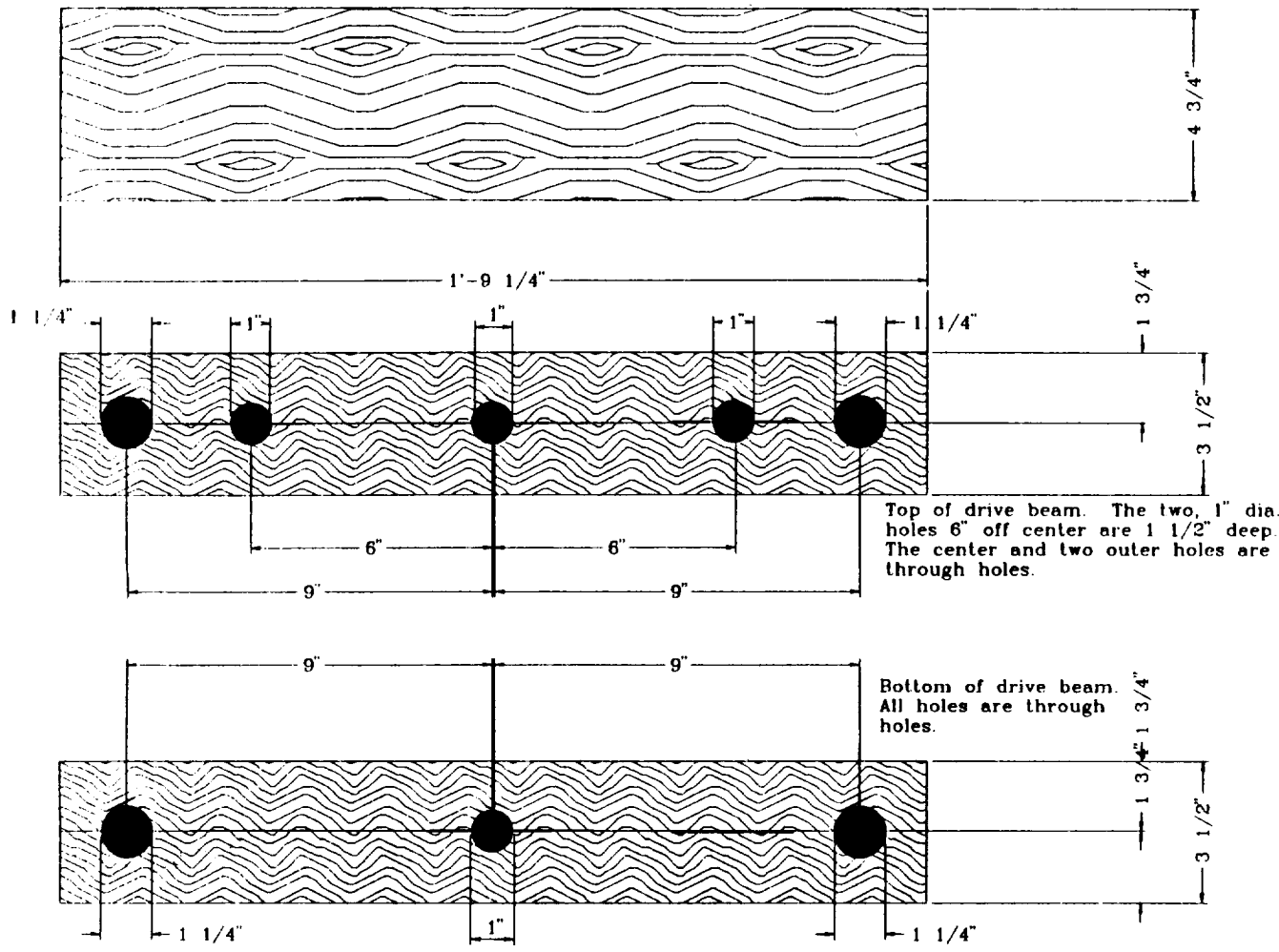

Figure 5. Construction of laminated oak drive beam.

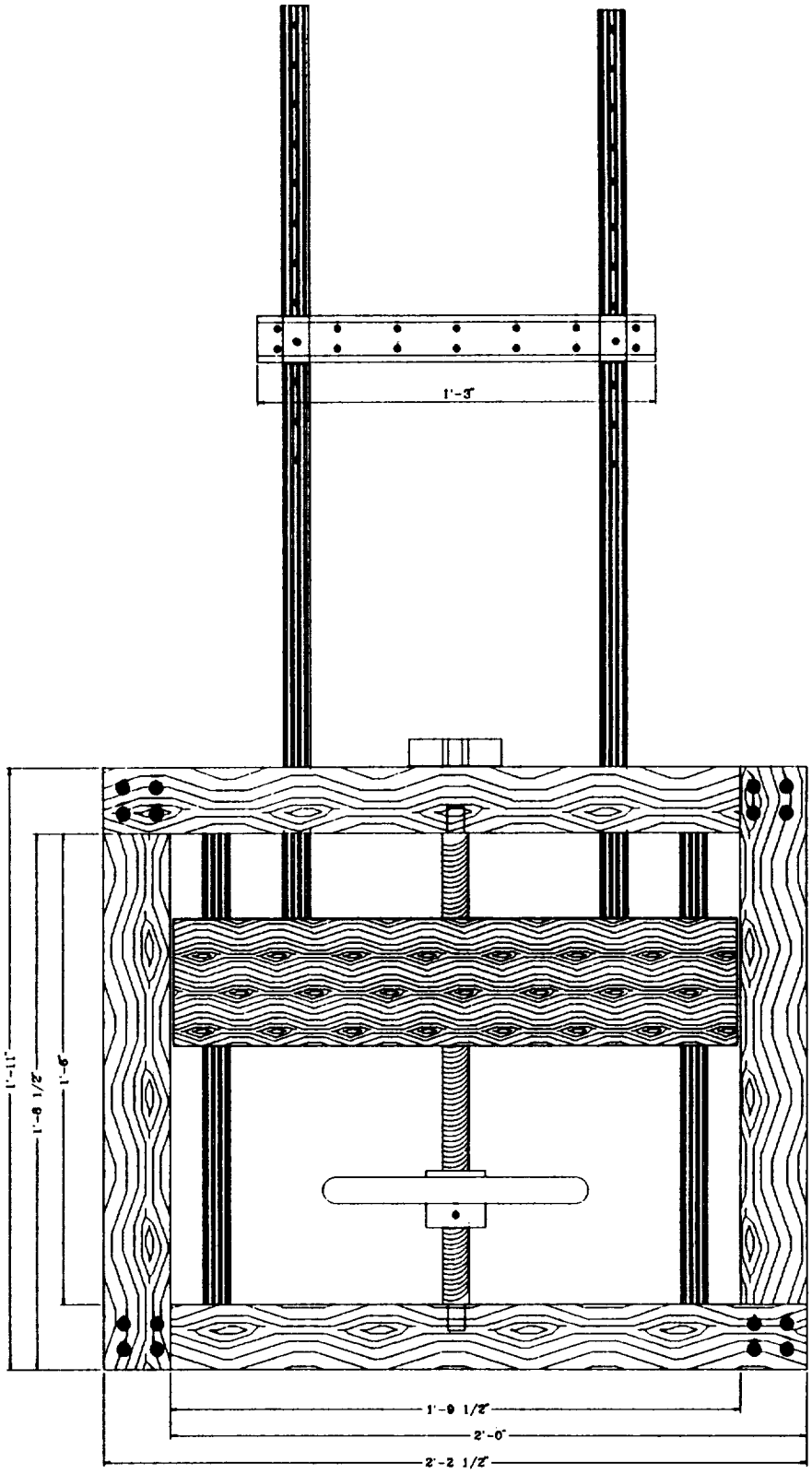

Figure 6. Maple frame with oak drive beam and Acme threaded rod. Two 1" diameter drive rods go up to the rail. The upper grip hangs from the rail while the lower grip screws into the load cell which is attached to the top of the frame by means of lag bolts.

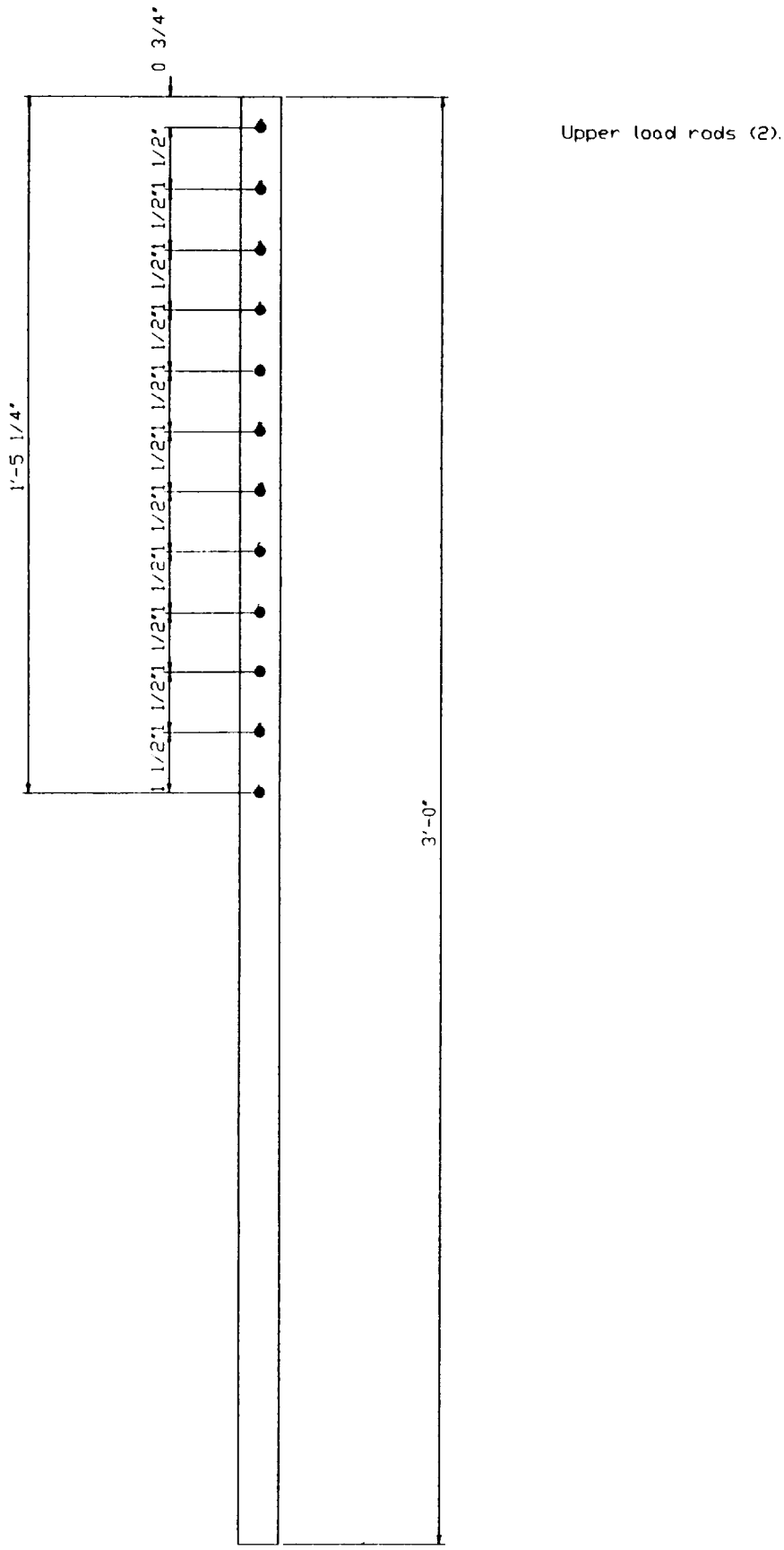

Figure 7. Drive rod (2) with drilled holes to accommodate 1/4" support pin.

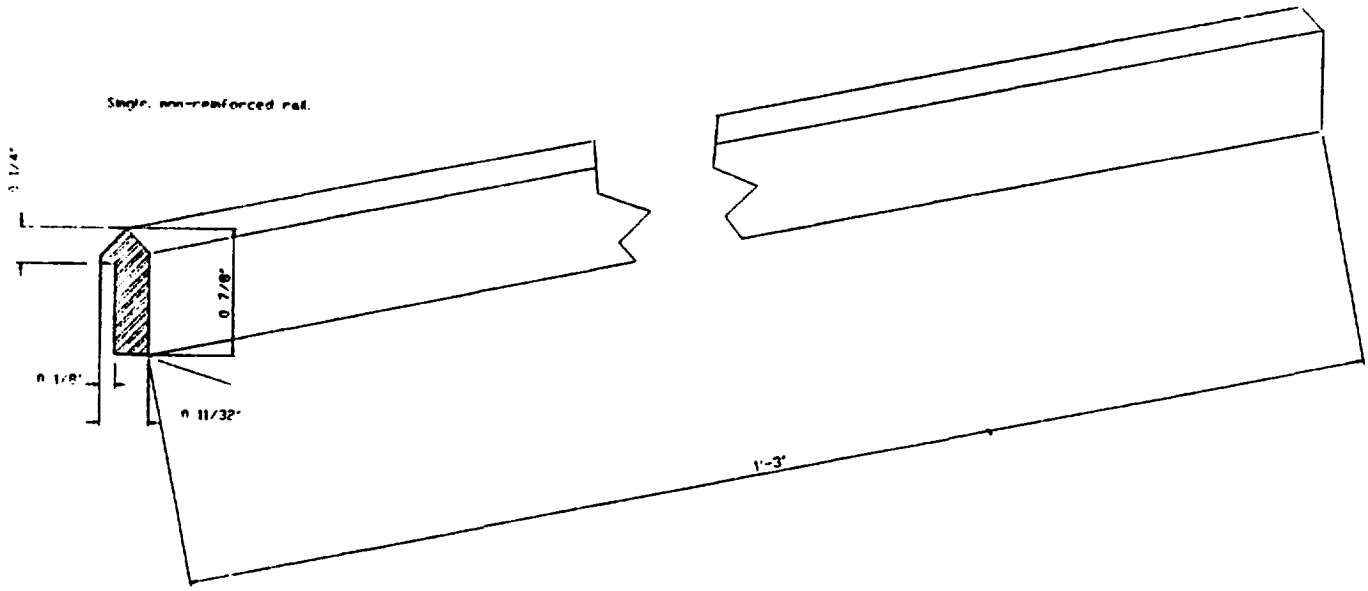

Figure 8. Single rail. Four are required.

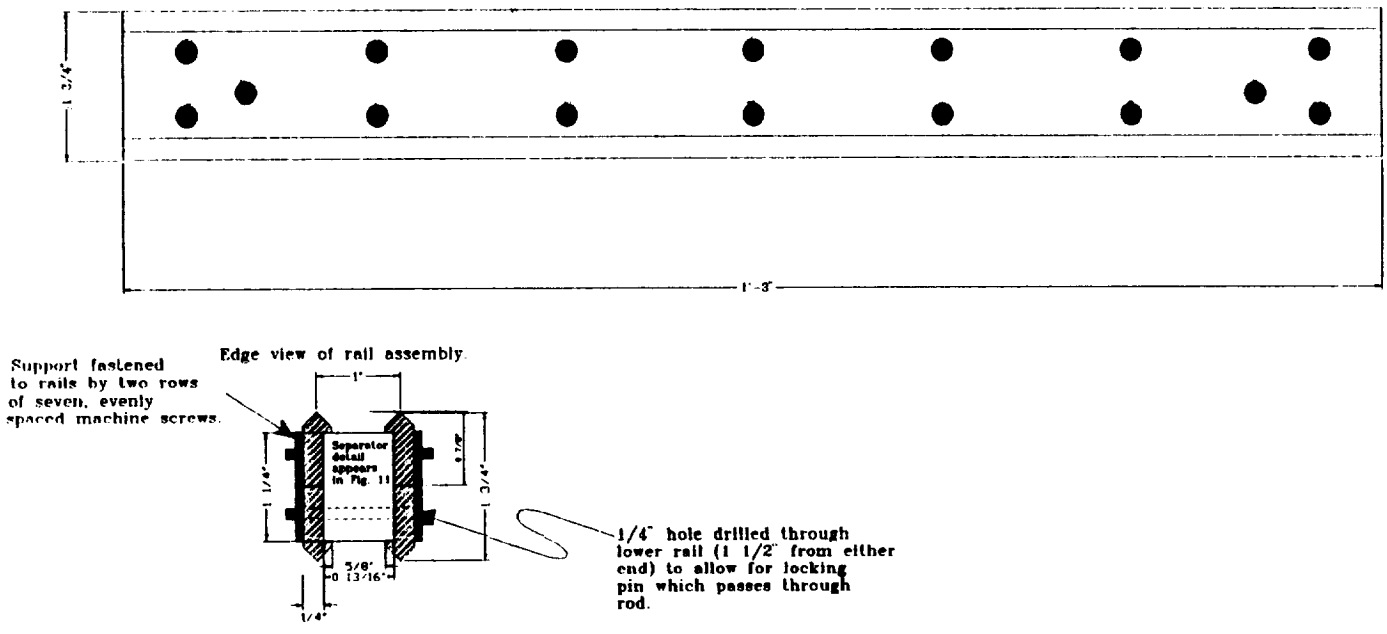

Figure 9. Rail assembly.

Rail separator detail.

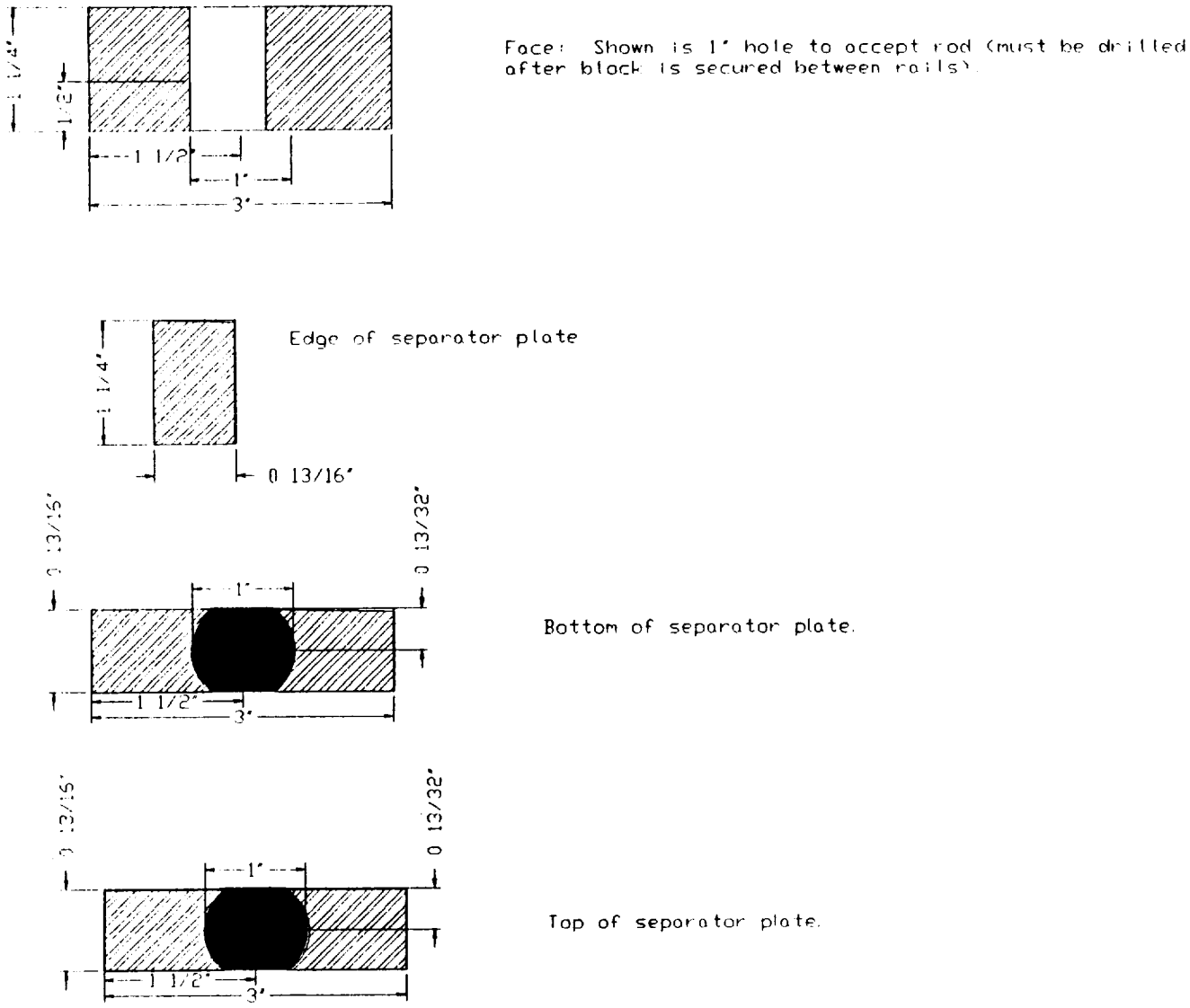

Figure 10. Detail of rail separator.

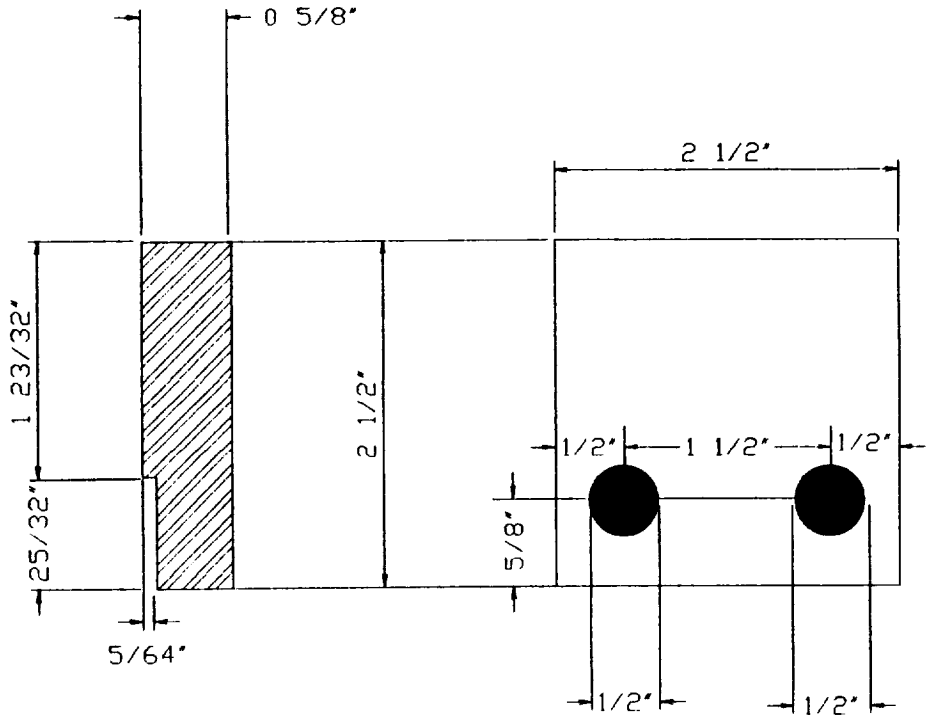

Figure 11. Gripping plate. Four are required.

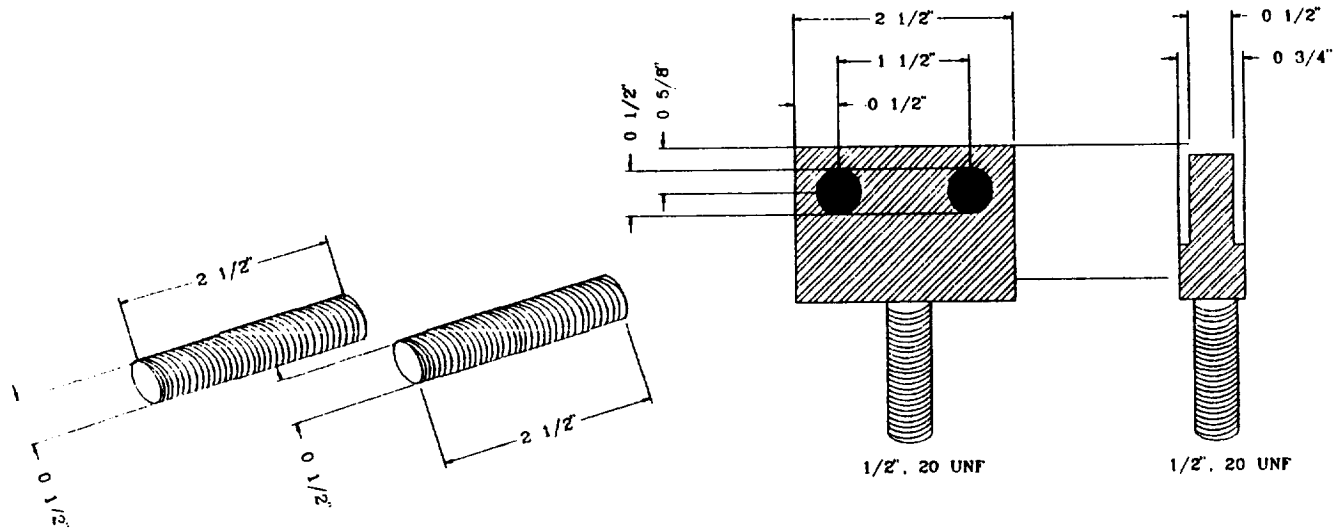

Figure 12. Bottom grip center plate. Two 1/2" dia. holes drilled through to allow passage of threaded rods. Gripping plates attach by nuts.

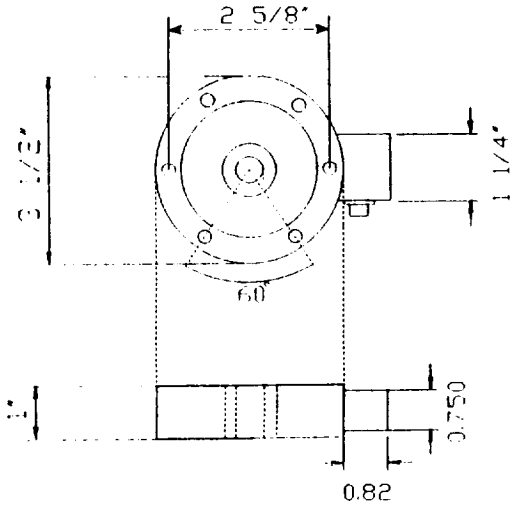

6 clearance holes equally spaced on 2.625" diameter B.C., 0.34" diameter thru.

Manufacturer's Specifications

Sensotec Model 41 Load Cell
Serial No. 296393
Part No. 572-05
Capacity: 0-5000 Lbs
Excitation Voltage: 10.0
T.C. Range: 60-160 degrees F.
Shunt Resistor Value: 59 kohms
Matching cable and connector (AA113)

With Amplifier:	%Capacity	Output
	0	0 volts
	50	2.5004 volts
	100	4.9996 volts
	50	2.5027
	0	0 volts

Figure 13. Sensotec load cell with manufacturer's specifications.

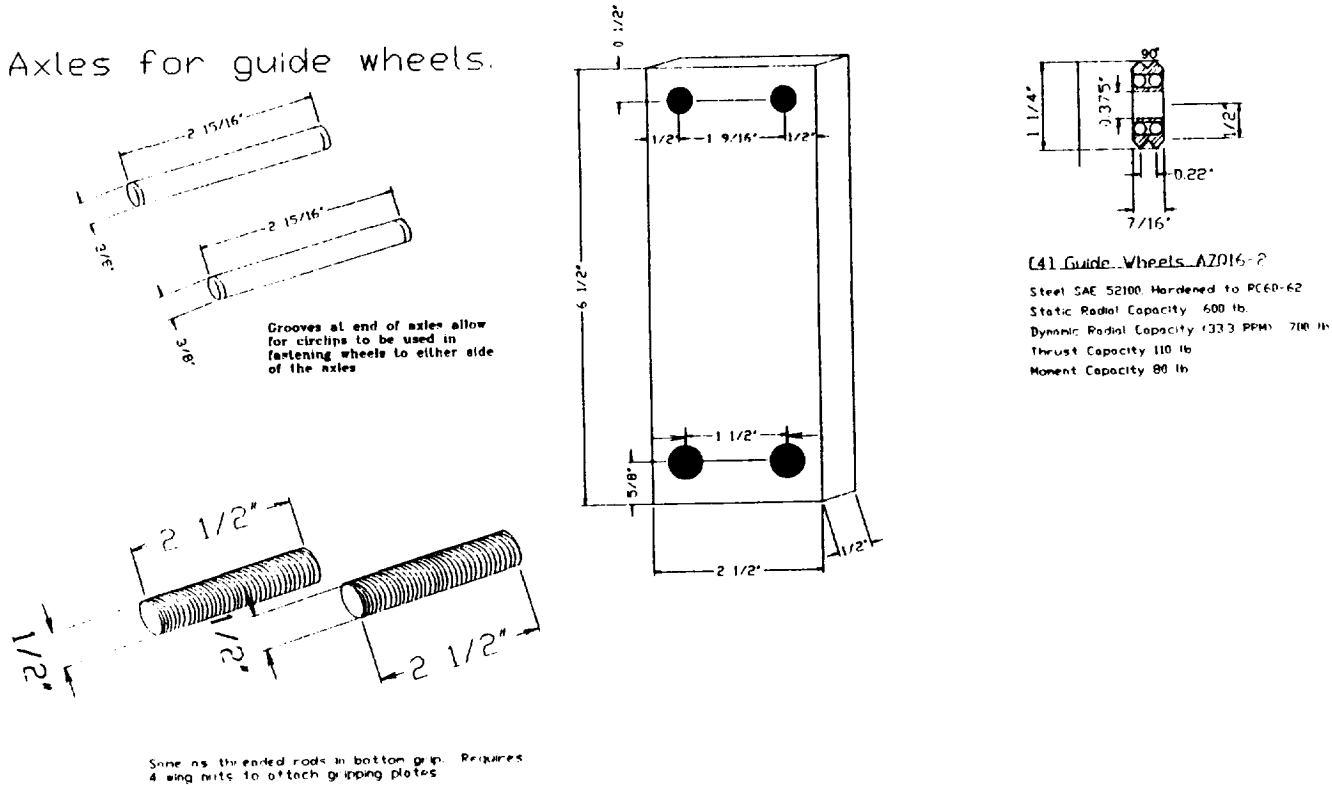

Figure 14. Shuttle assembly for upper grip.

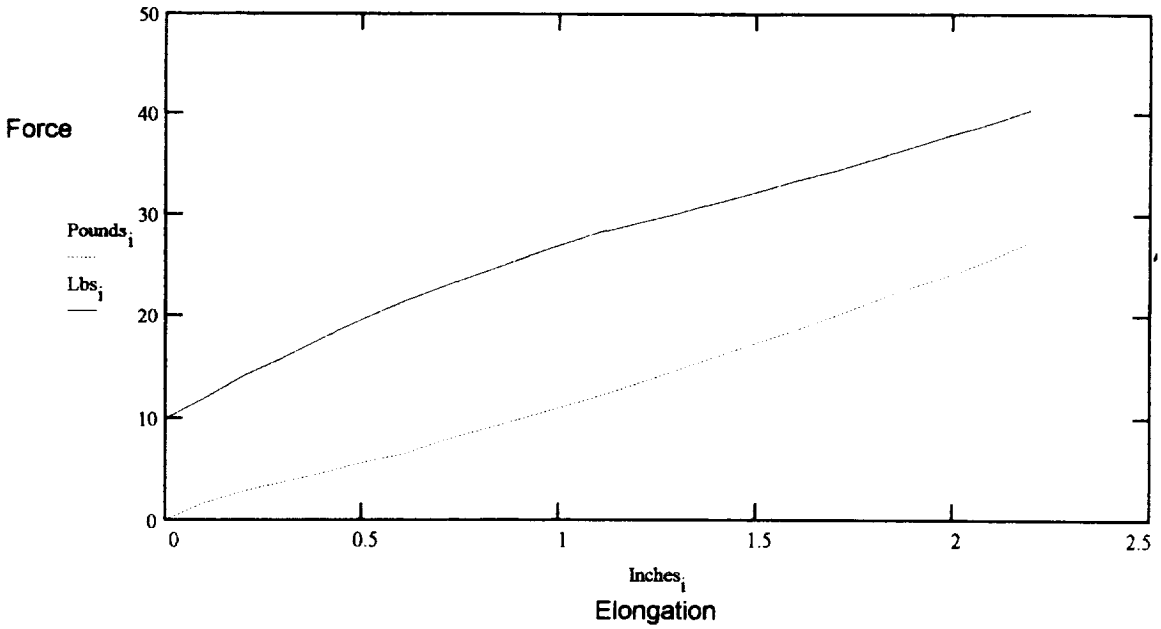

Figure 15. Neat samples of Ferris See-thru tested on Chatillon {Pounds} and hand operated device {lbs} using load cell manufacturer's specifications.

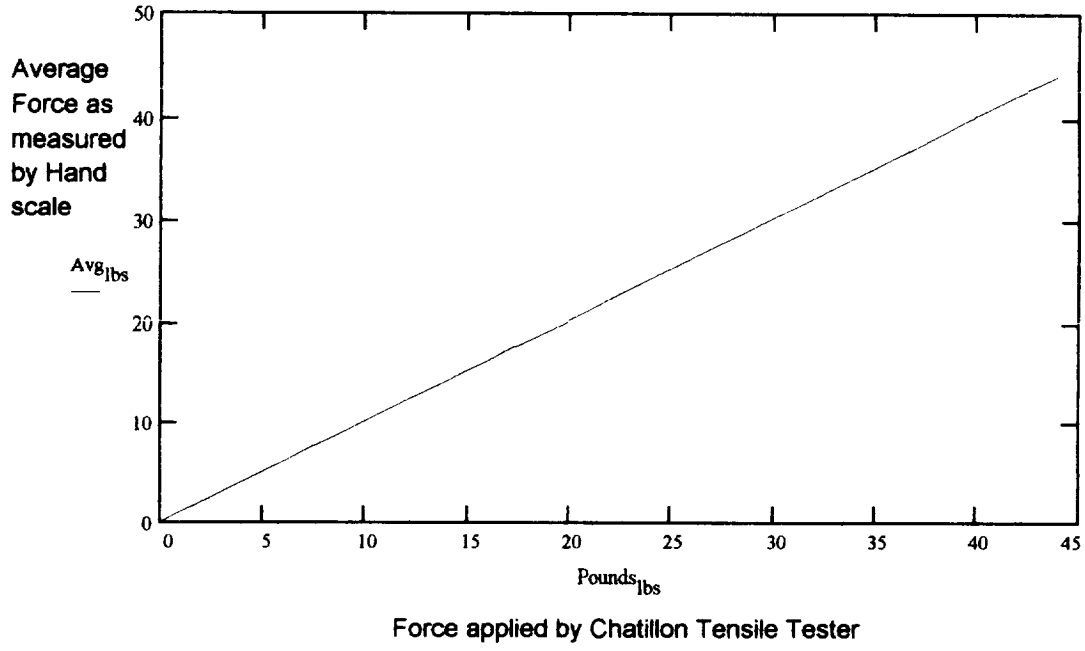

Figure 16. Average reading of hand scale (Chatillon Model IN-50) for ten trials, 0 - 44 pounds on Chatillon Tensile Tester.

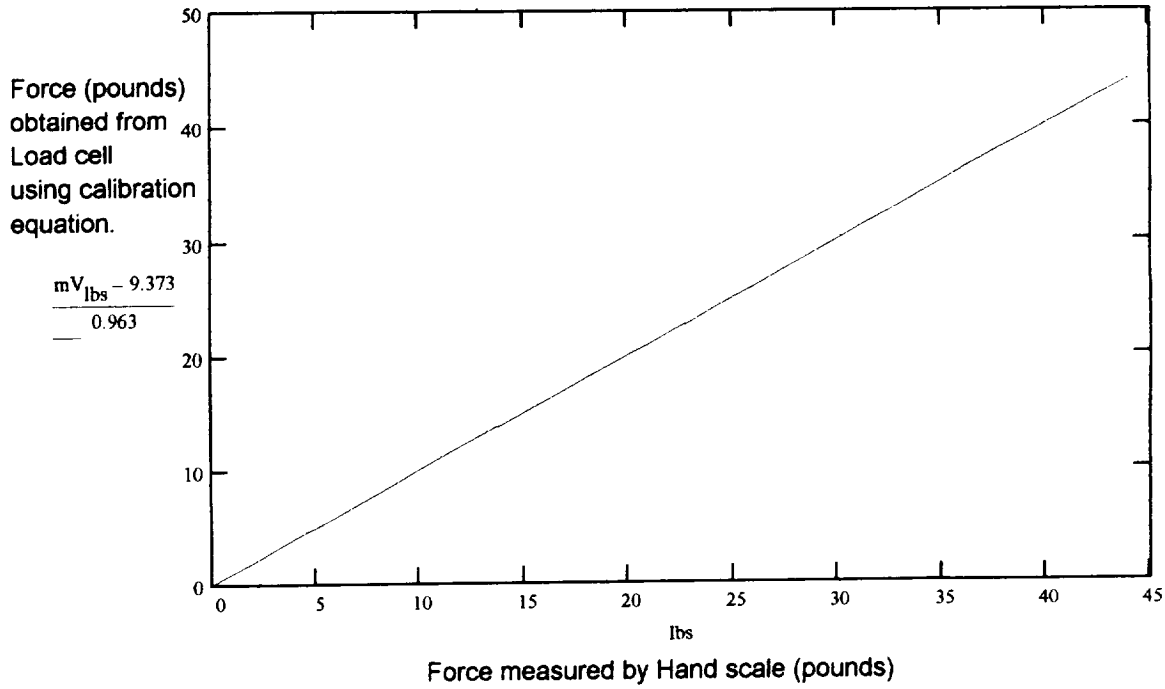

Figure 17. Calibration of load cell using Chatillon Model IN-50 Hand Scale. The load cell's average output in millivolts for ten trials is plotted against the hand scale's reading in pounds. The relationship between the load cell's output in millivolts to the force applied was determined to be. . .

$$Lbf = \frac{mV - mV_0}{0.963}$$

mV = reading in milli-volts

mV_0 = initial reading [millivolts]

Lbf = Pounds force

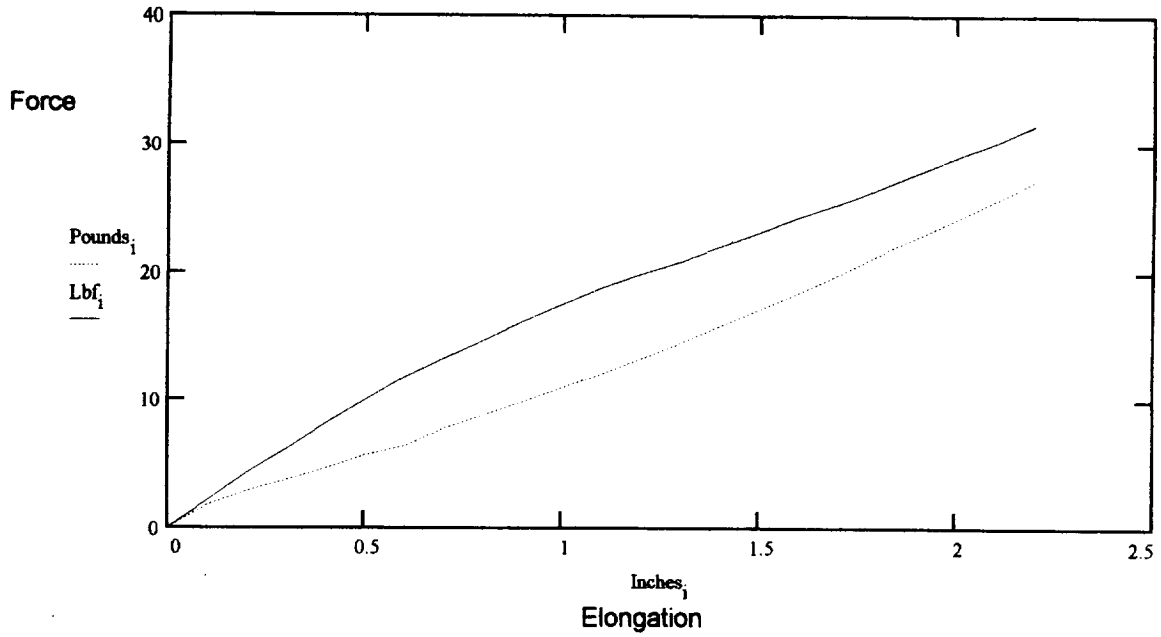

Figure 18. Neat samples of Ferris See-thru tested on Chatillon {pounds} and hand operated device (Lbf) using calibration data.

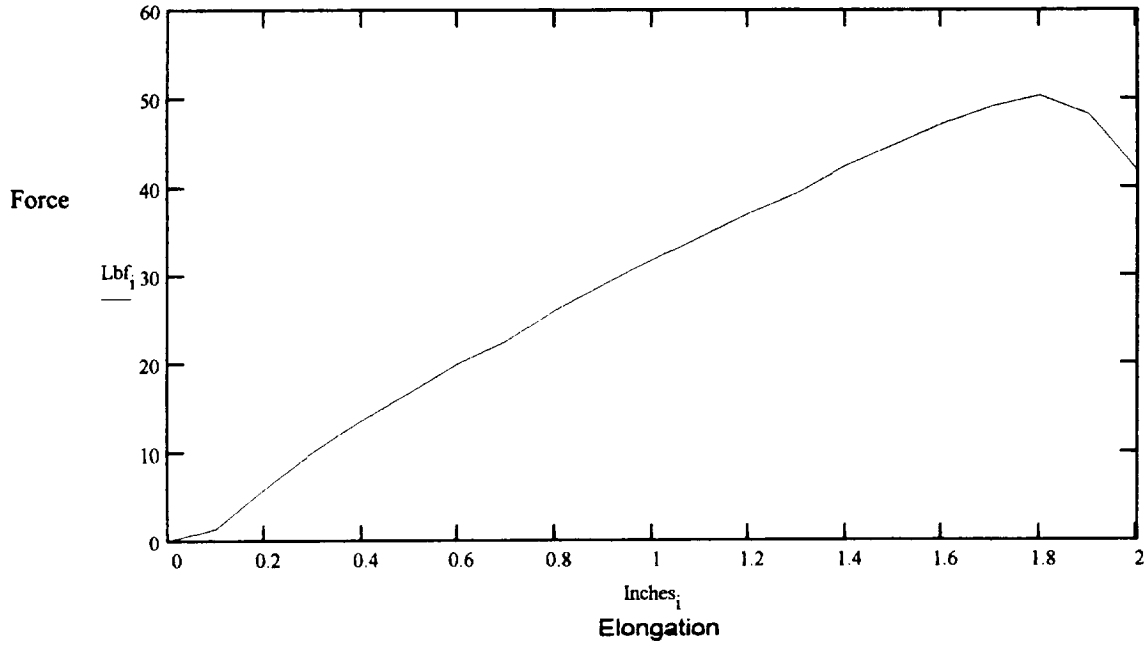

Figure 19. Force vs. elongation for Ferris See-thru Neat (0716931).

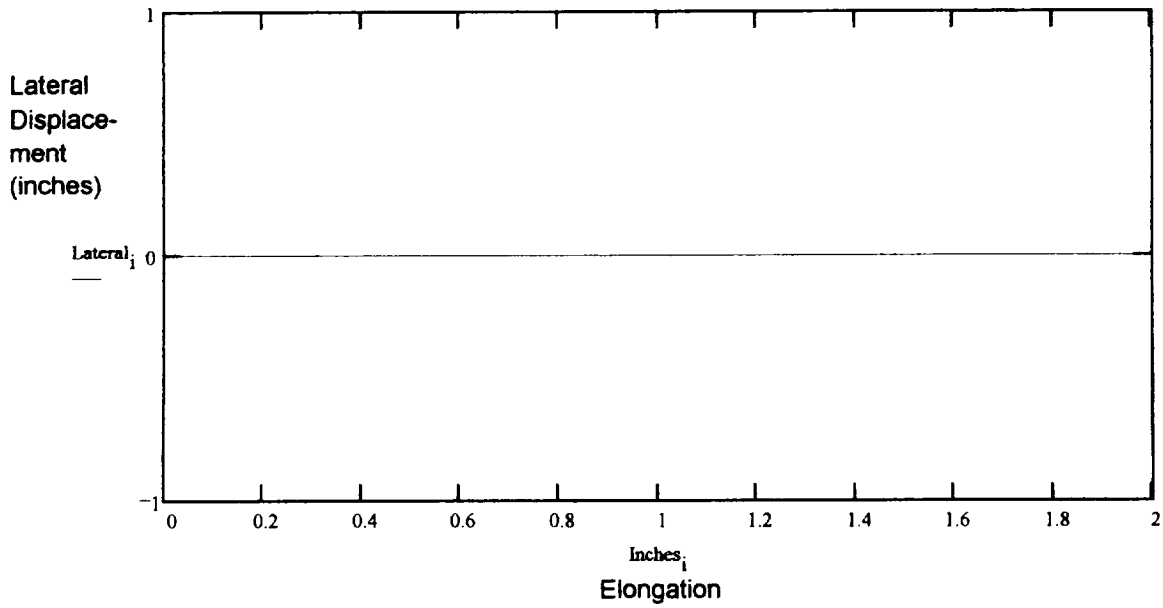

Figure 20. Lateral displacement vs. elongation for Ferris See-thru Neat (0716931).

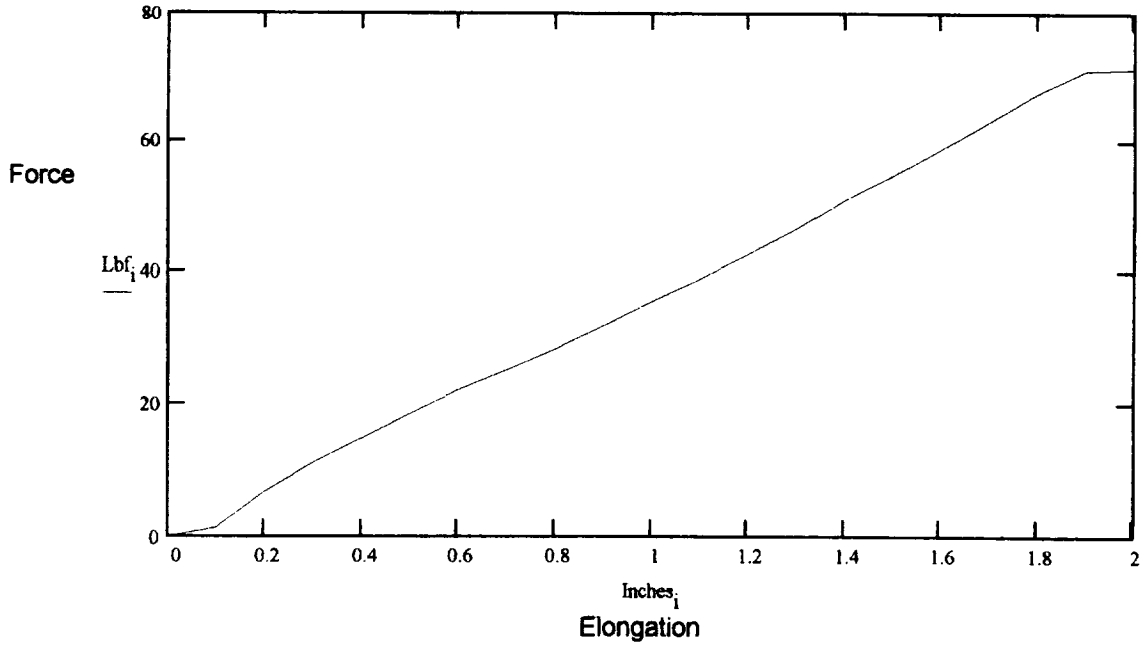

Figure 21. Force vs. elongation for Ferris See-thru Al 0° (0716932).

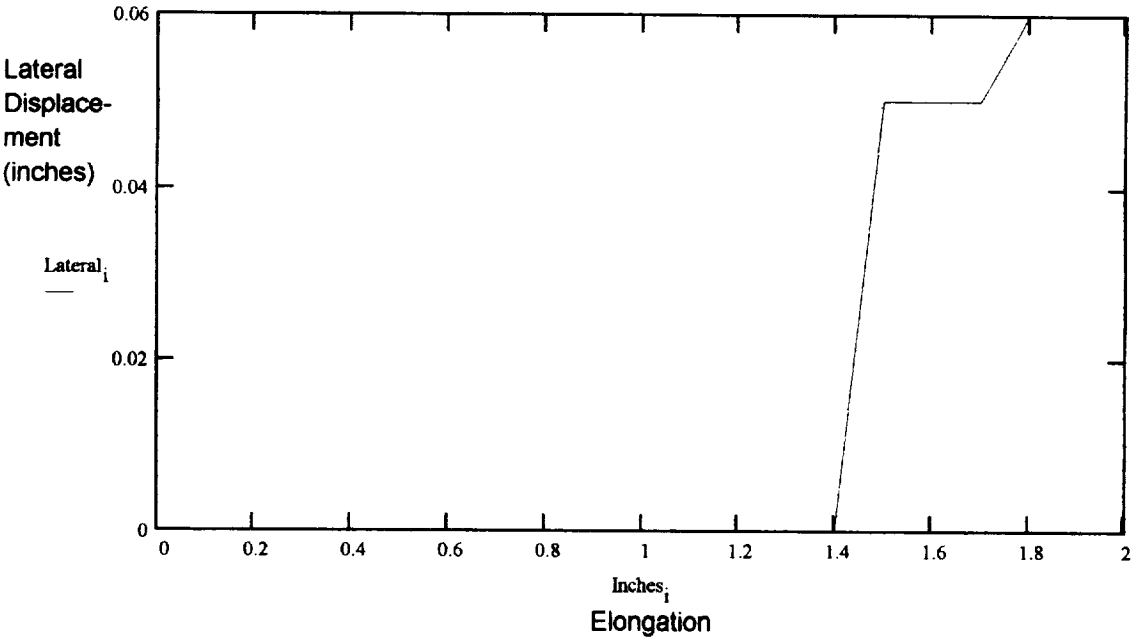

Figure 22. Lateral displacement vs. elongation for Ferris See-thru Al 0° (0716932).

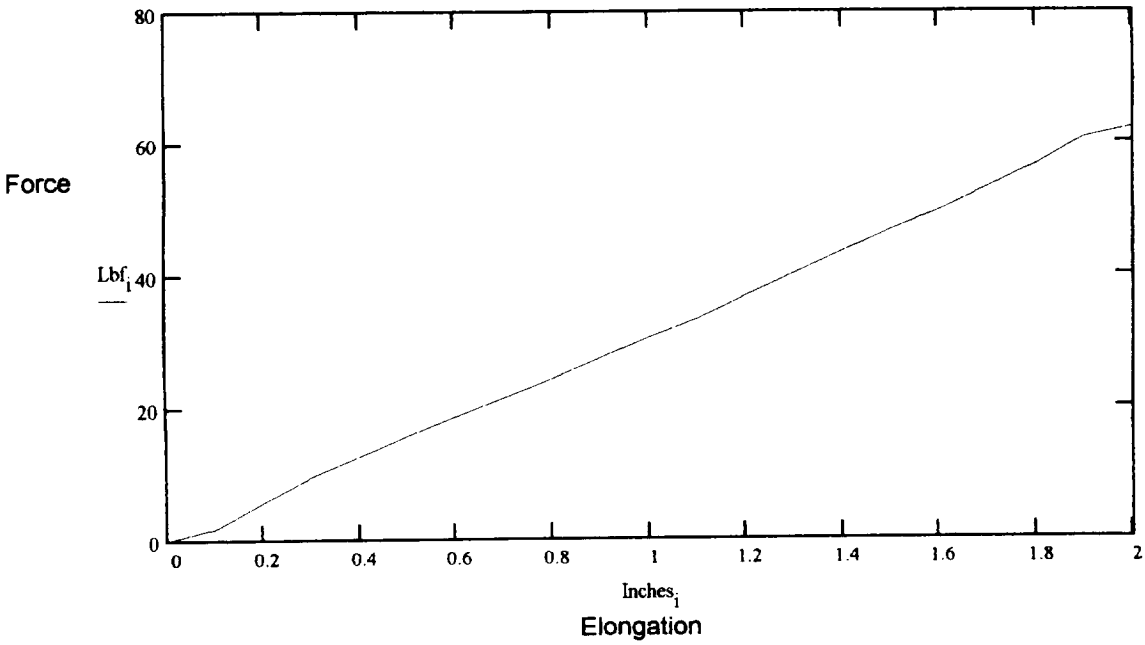

Figure 23. Force vs. elongation for Ferris See-thru Al 30° (0716933).

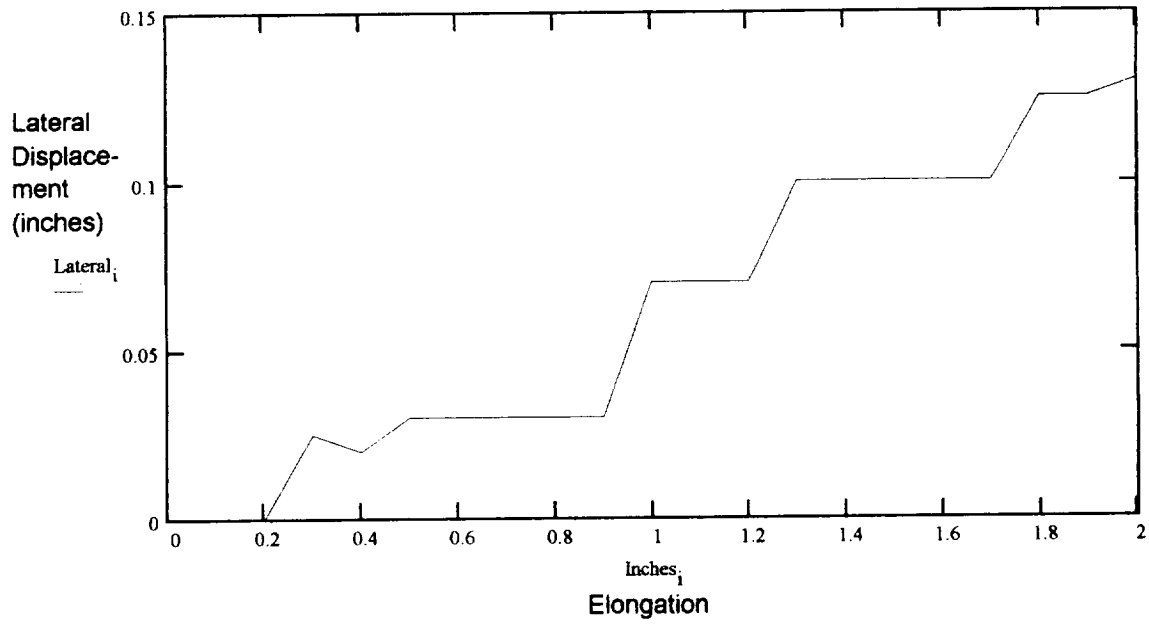

Figure 24. Lateral displacement vs. elongation for Ferris See-thru Al 30° (0716933).

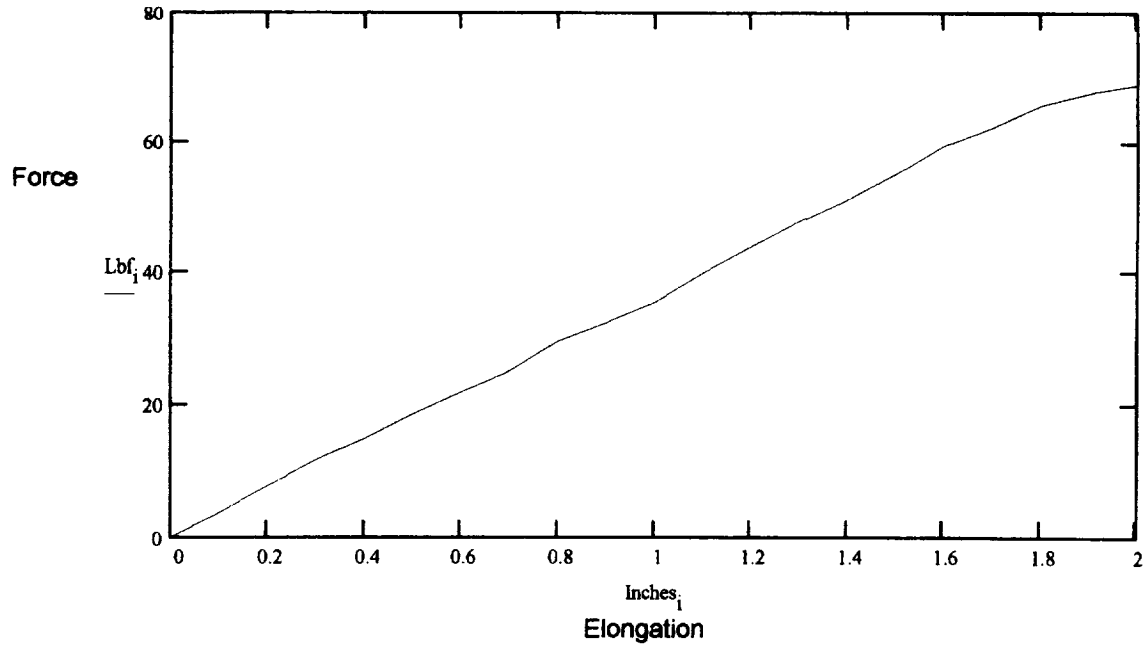

Figure 25. Force vs. elongation for Ferris See-thru Al 45° (0716934).

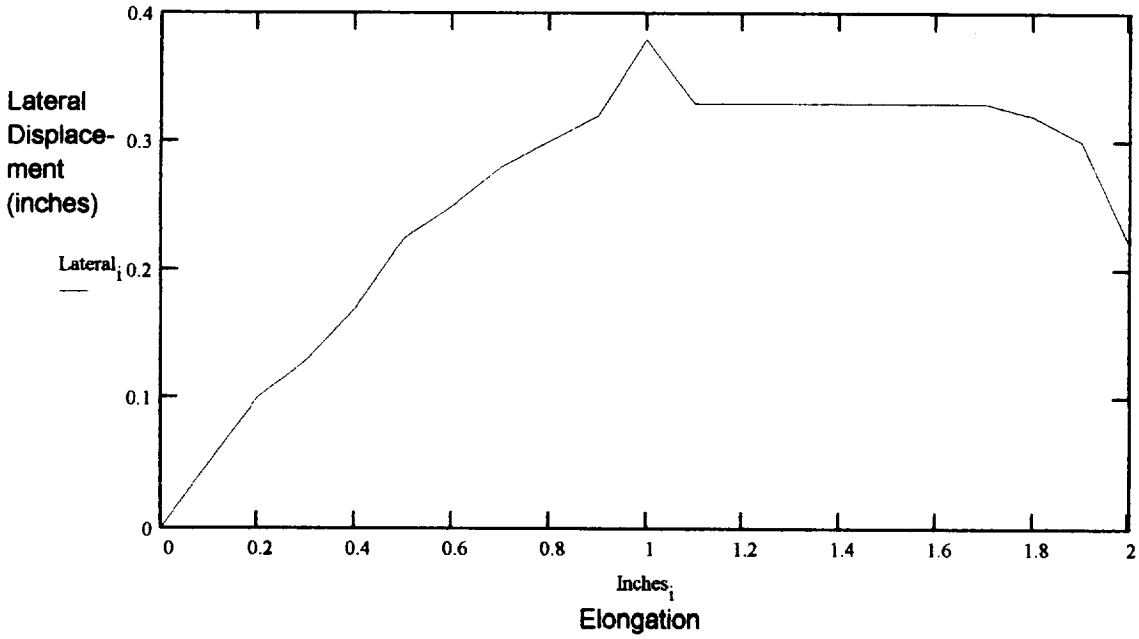

Figure 26. Lateral displacement vs. elongation for Ferris See-thru Al 45° (0716934).

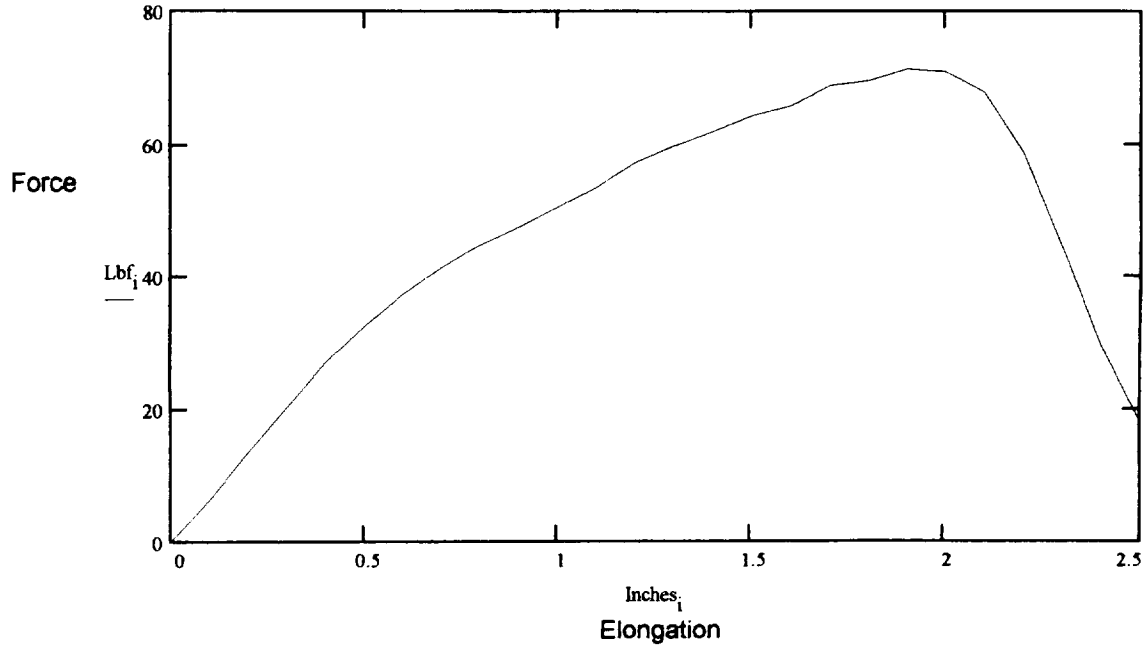

Figure 27. Force vs. elongation for Ferris See-thru Al 60° (0716935).

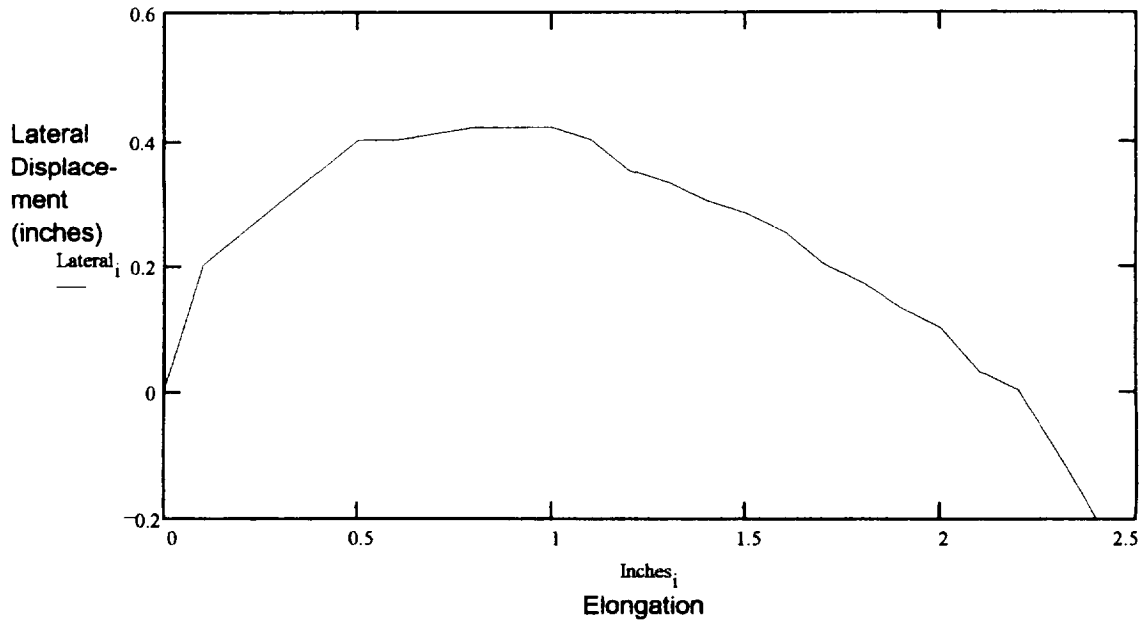

Figure 28. Lateral displacement vs. elongation for Ferris See-thru Al 60° (0716935).

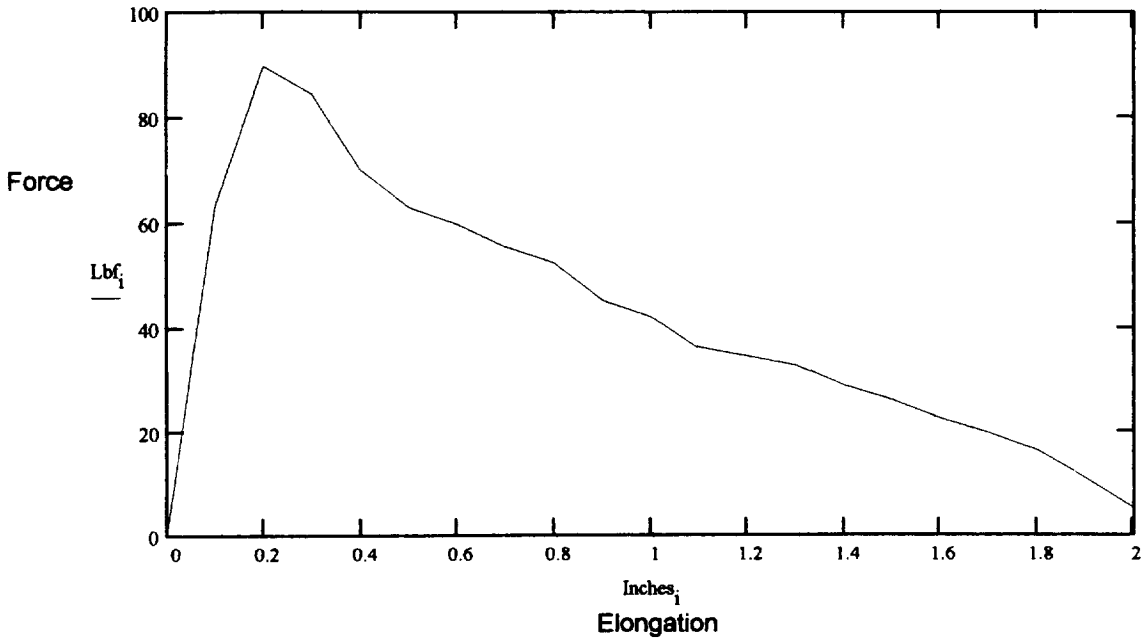

Figure 29. Force vs. elongation for Ferris See-thru Al 90° (0716936).

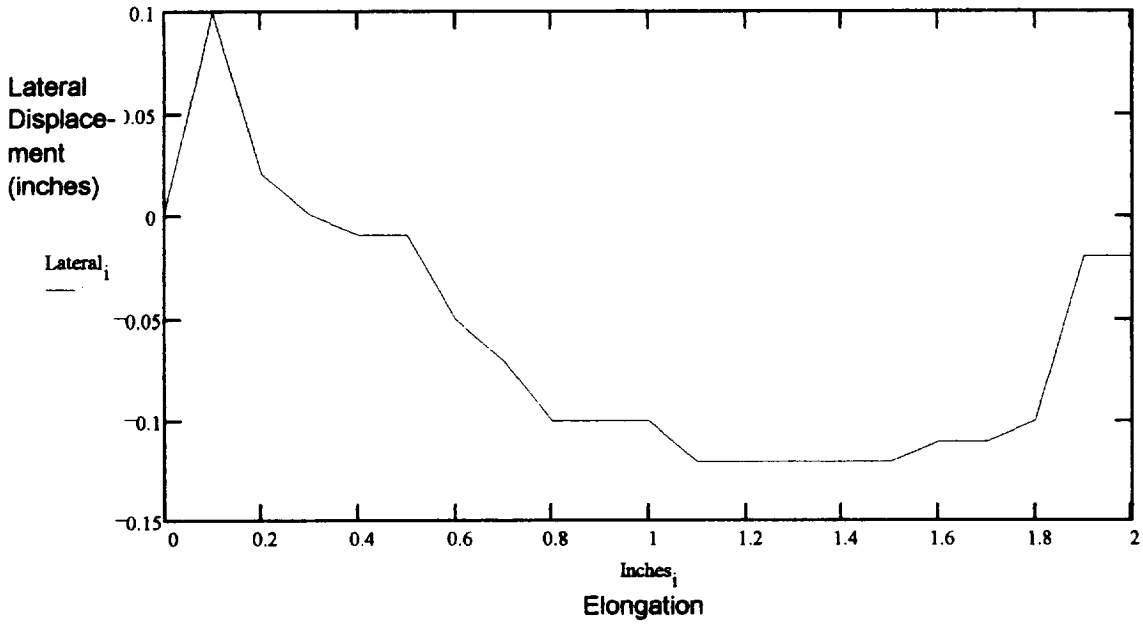

Figure 30. Lateral displacement vs. elongation for Ferris See-thru Al 90° (0716936).

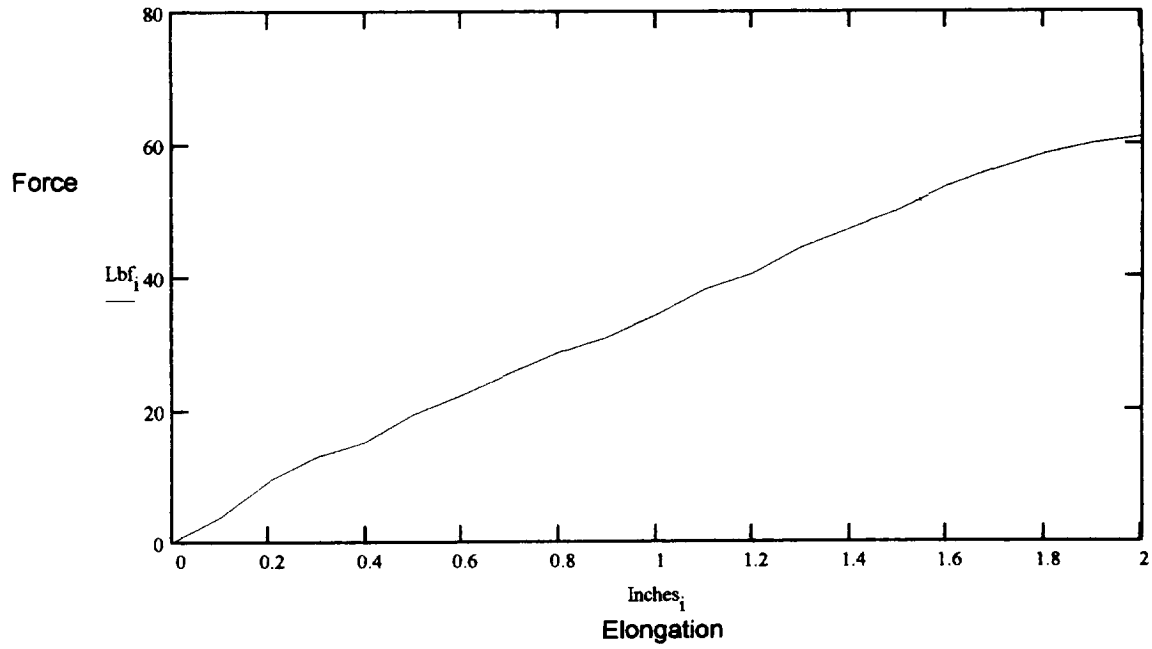

Figure 31. Force vs. elongation for Ferris See-thru Fiberglass 0° (0716937).

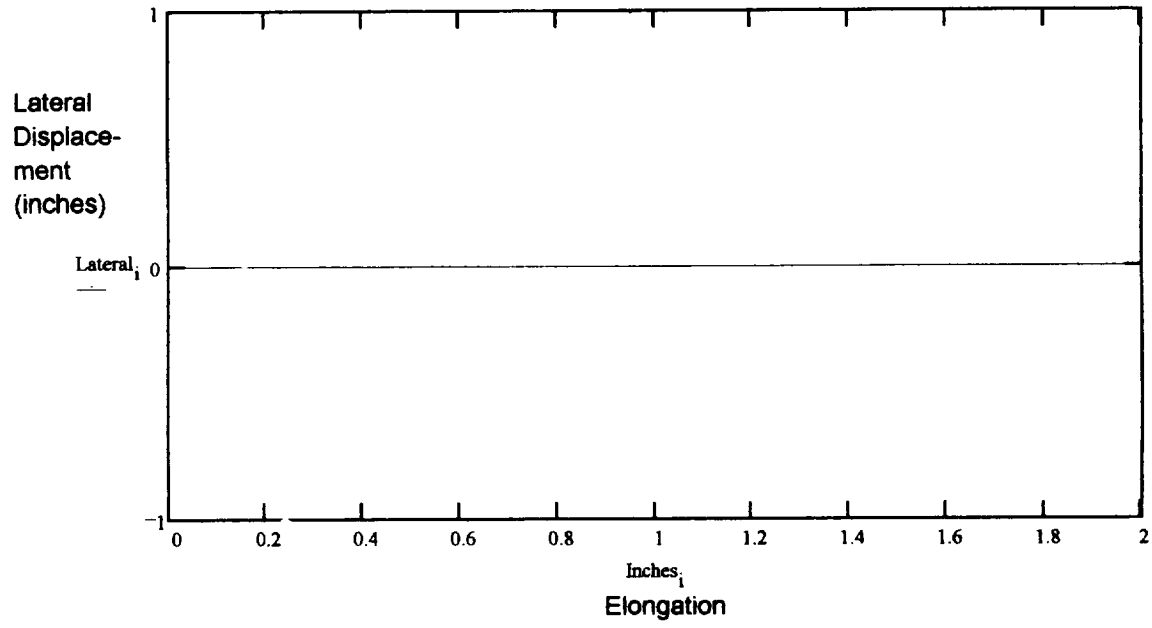

Figure 32. Lateral displacement vs. elongation for Ferris See-thru Fiberglass 0° (0716937).

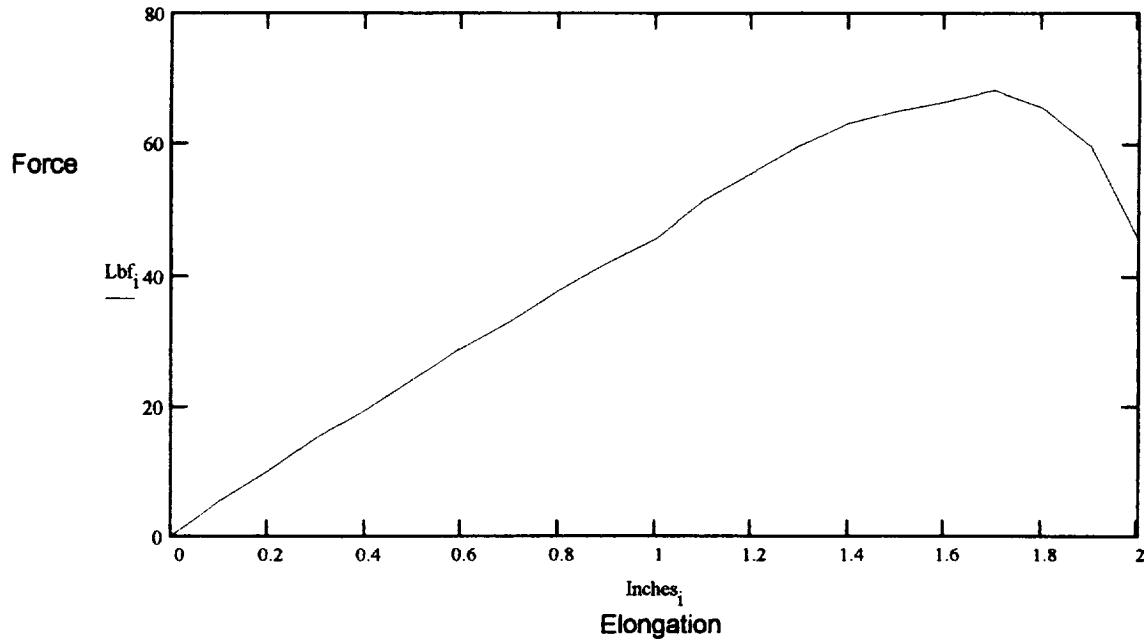

Figure 33. Force vs. elongation for Ferris See-thru Fiberglass 30° (0716938).

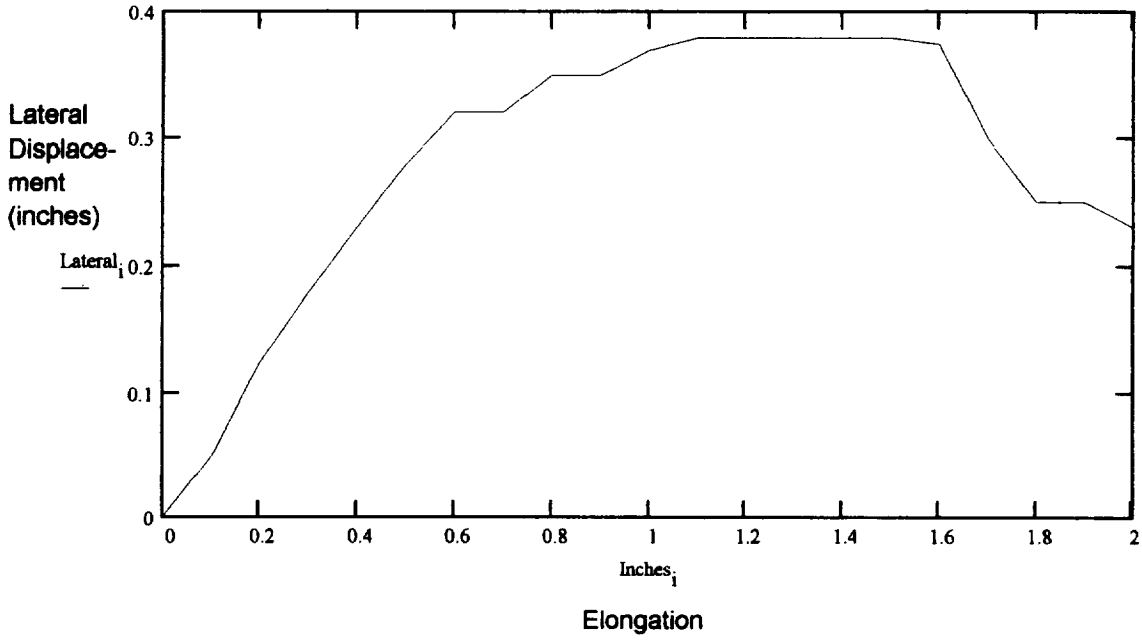

Figure 34. Lateral displacement vs. elongation for Ferris See-thru Fiberglass 30° (0716938).

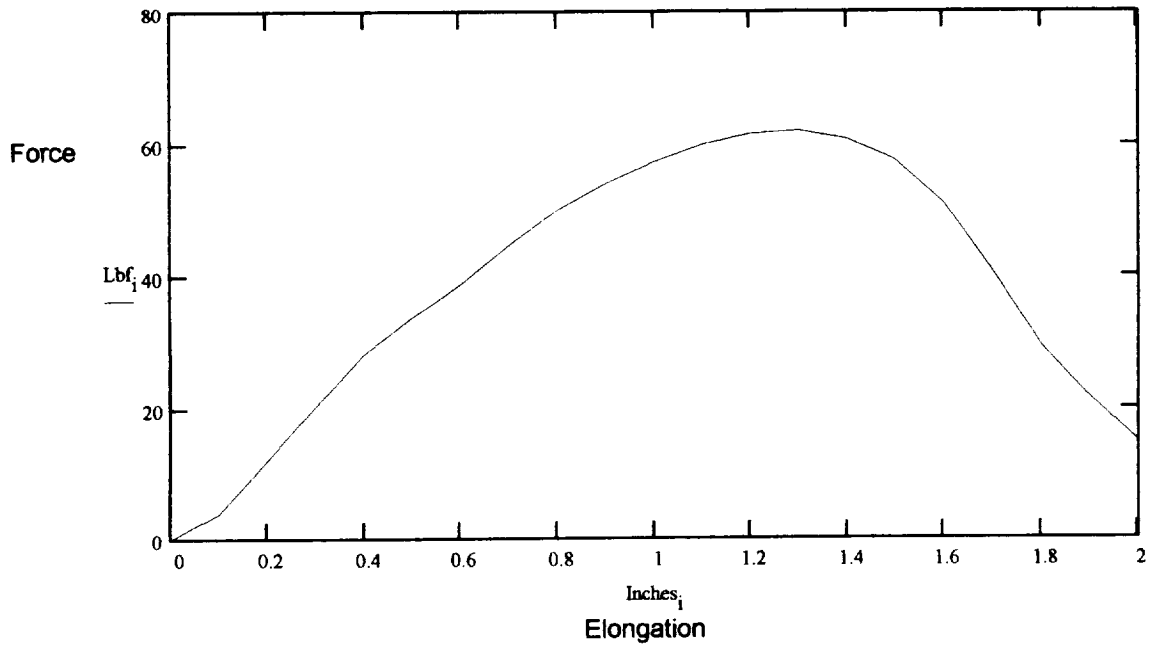

Figure 35. Force vs. elongation for Ferris See-thru Fiberglass 45° (0716939).

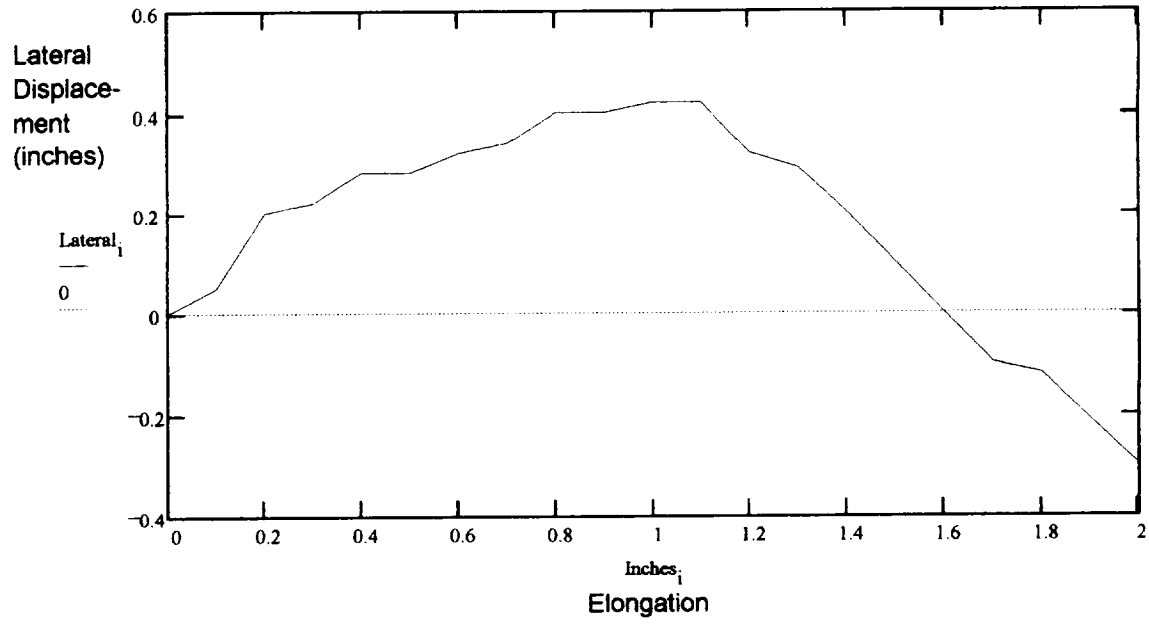

Figure 36. Lateral displacement vs. elongation for Ferris See-thru Fiberglass 45° (0716939).

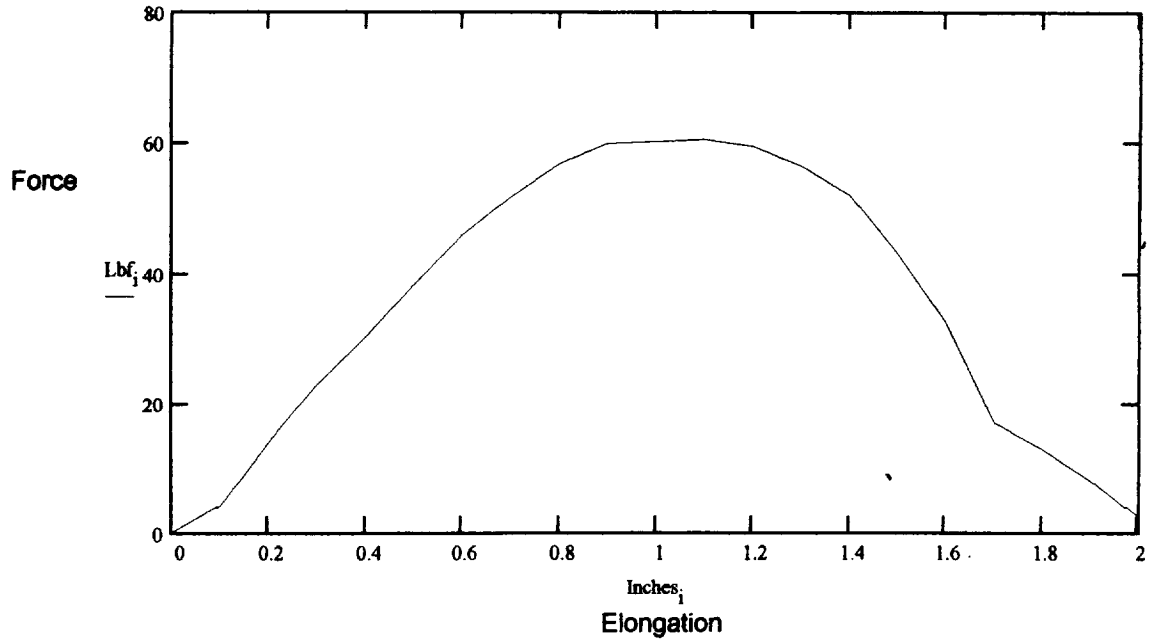

Figure 37. Force vs. elongation for Ferris See-thru Fiberglass 60° (07169310).

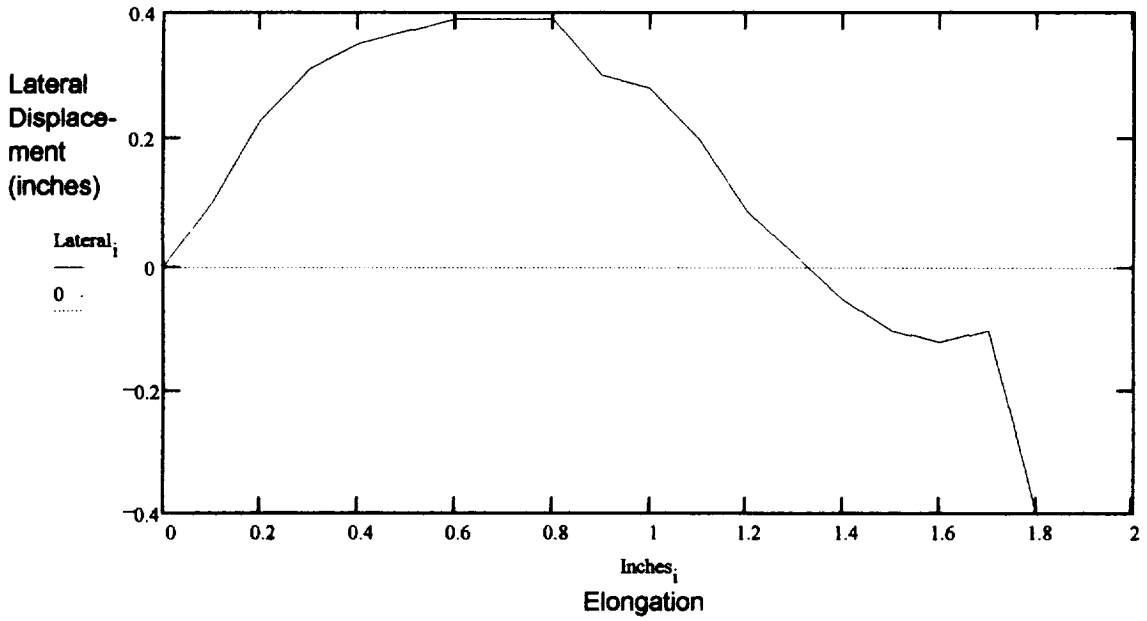

Figure 38. Lateral displacement vs. elongation for Ferris See-thru Fiberglass 60° (07169310).

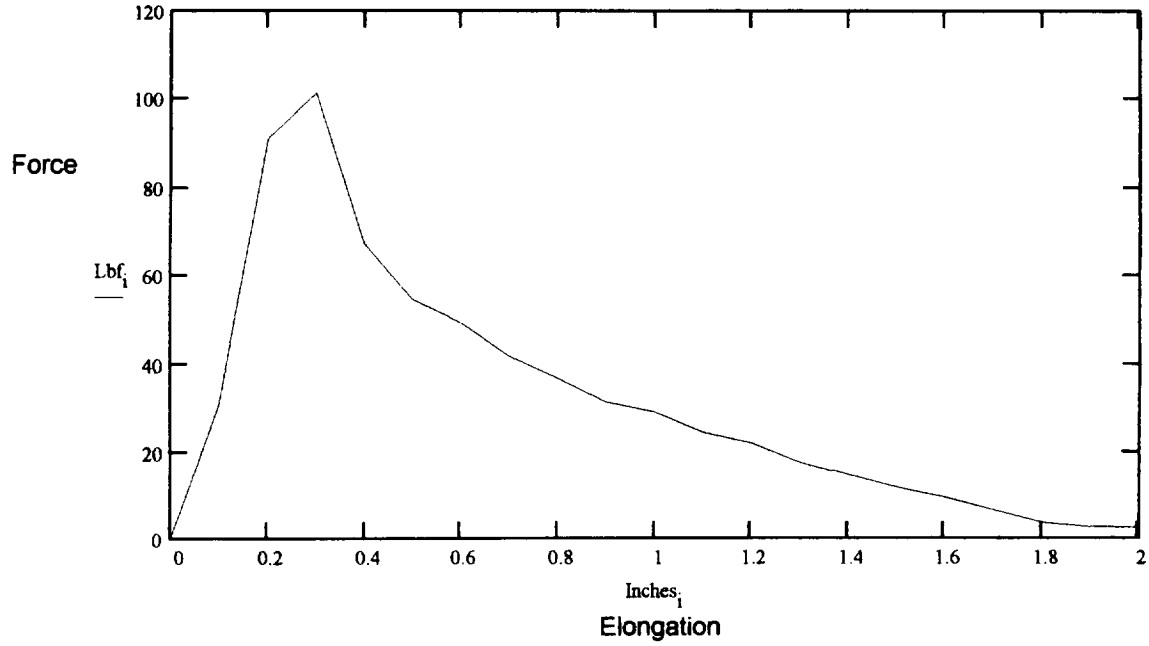

Figure 39. Force vs. elongation for Ferris See-thru Fiberglass 90° (07169311).

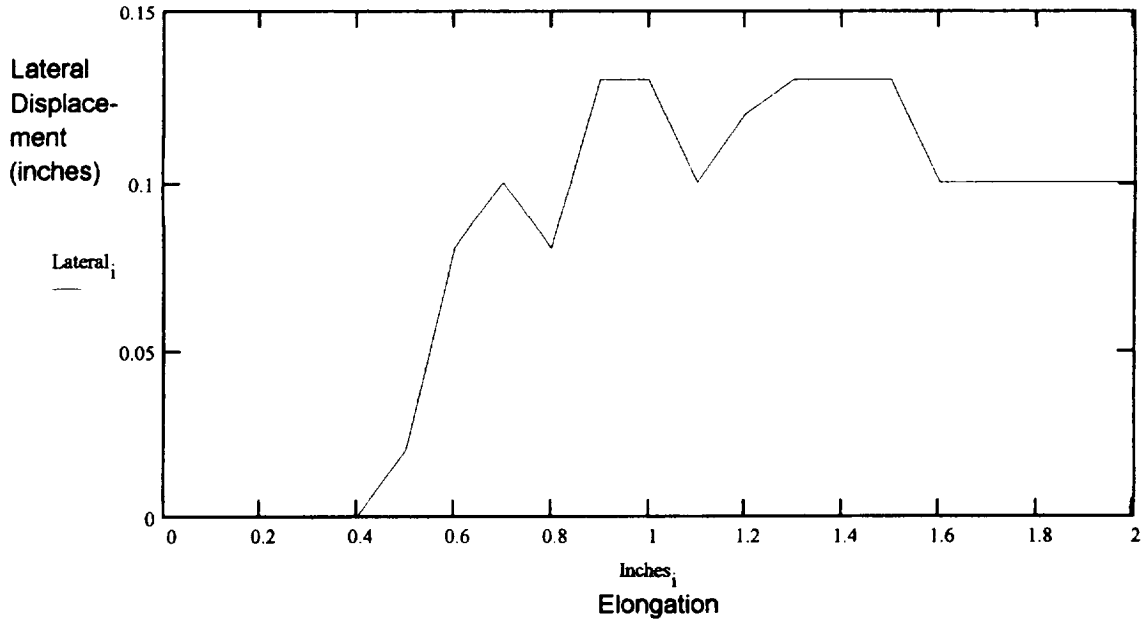

Figure 40. Lateral displacement vs. elongation for Ferris See-thru Fiberglass 90° (07169311).

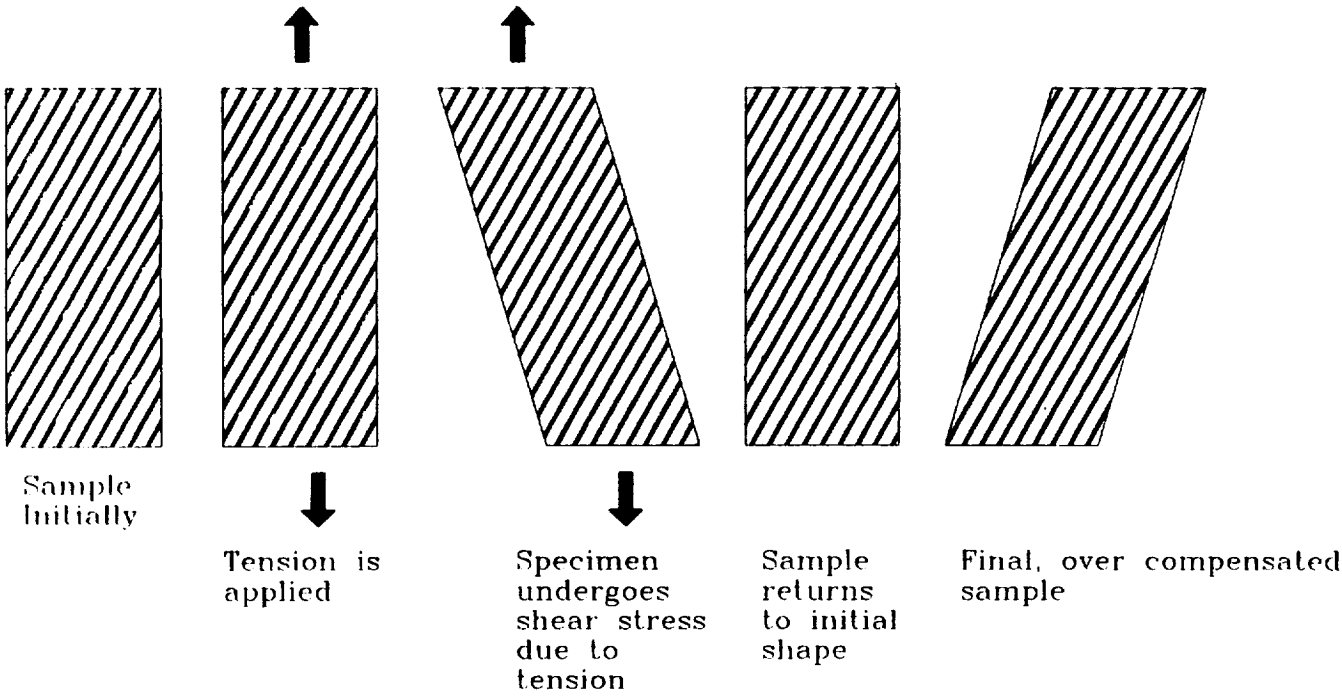

Figure 41. Schematic of sample deformation.

References

1. Penniman, Charles F.: The First Materials Testing in America. ASTM Standardization News. January, 1991

2. Hull, Derek An Introduction to Composite Materials Cambridge University Press (1981)

3. Fellers, William O. Materials Science, Testing, and Properties for Technicians Prentice Hall, copyright 1990

4. Wampler, M. D., Spiegel, F. X. and West, H. A. Continuous Unidirectional Fiber Reinforced Composites: Fabrication and Testing Journal of Materials Education, Vol. 14, pp. 293-301, 1992.

5. West, Harvey A., Sprecher, A. F. Fiber Reinforced Composite Materials National Educators' Workshop: Update '90, NIST Special Publication 882 (1991).

6. Askeland, Donald R., The Science of Engineering Materials, Second Edition PWS-Kent Publishing Company (1984).

7. Agarwal, Bhagwan D., Broutman, Lawrence J. Analysis and Performance of Fiber Composites, Second Edition John Wiley & Sons, 1990

8. Larsen, Carl G.: Design Considerations for Materials Testing Tension/Compression Grips. MTS Systems Corporation Minneapolis, Minnesota

9. Georgeson, Gary & Milstein, Frederick: Load and Fixture for Uniform Plastic Deformation Single Crystals. Rev. Sci. Instrum. 54 (8), August, 1983

10. Perlov, Anatoly & Martin, James: Calibration and Verification of Materials Testing Machines and Systems. ASTM Standardization News. January, 1991

11. Sterling Instrument Handbook of Design Components. Sterling Instrument, 2101 Jericho Turnpike, New Hyde Park, N.Y. 11042-5416